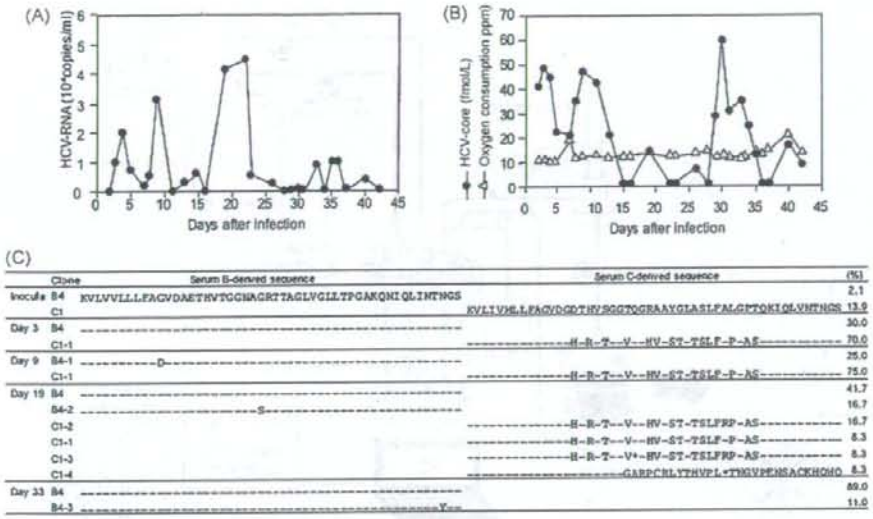

Fig. 3. HCV propagation in FLC4 cells cultured in the RFB system following inoculation with pooled sera obtained from HCV carriers. The 3D-cultured FLC4 cells were incubated with a pooled serum sample for 12 h, followed by changing the culture medium to fresh one. Culture medium was periodically collected for 42 days after inoculation, and HCV RNA and the viral core protein were quantified, respectively, by real-time RT-PCR and ELISA. (A) HCV RNA level in culture supernatant. (B) HCV-core protein (closed circles) and oxygen consumption (open triangles) levels in culture supernatant. (C) Changes in the viral quasispecies distribution after the inoculation. Percentages in the inoculum or in the culture medium at each time point (day 3, 9, 19, or 33 p.i.) are indicated at the right side. *, termination codon.

mL RFB column, as estimated from the glucose consumption (Kawada et al., 1998). Culture medium in the RFB was replaced with fresh medium 12 h post-infection (p.i.) and periodically sampled for 42 days.

Fig. 3A and B shows the levels of HCV RNA and viral core protein in the culture medium, respectively. HCV RNA was not observed on the first 2 days following infection, but was detectable from day 3 p.i. Viral RNA levels fluctuated, with peaks on days 3, 9, 19–21 and 33–36 p.i. At days 19–21 p.i., the average amount of HCV RNA detected in the culture supernatant was approximately 3×10^6 copies/day. Intermittent peaks were observed in HCV core protein levels in the culture supernatant, and the peak pattern of the core protein was largely consistent with that of viral RNA. During the infection experiment, the level of oxygen consumption was constant at approximately 12 ppm, thus suggesting that the desired conditions (constant or very gradually increasing cell number) were maintained.

3.3. Quasispecies analysis in RFB culture

The above results suggest that, although the environment was consistent in the pooled serum infection, there were periods in which the viruses actively replicated and released from the cells and periods in which they poorly replicated. The pooled serum used for the infection exhibited HCV populations had at least 26 distinct quasispecies (Table 1). To investigate whether the quasispecies distribution was altered due to infection, and whether HCV populations are selected during long-term culture in the RFB, total RNA was extracted from the culture supernatant samples collected on days 3, 9, 19 and 33 p.i., and the nucleotide sequence of the region containing HVR1 was determined, as described above. As shown in Fig. 3C, it is of interest that only two HCV species were detected in the sample at day 3 p.i.; the dominant clone C1-1, comprising approximately 70% of the viral population, and clone B4, comprising 30%. Although clone C1-1 was not detected in the sequence of the inoculum shown in Table 1, it was most similar to clone C1, a dominant clone in plasma C, among the HCV population observed in the inoculum; thus, it is possible that clone C1-1 is one of the minor species in serum C. Clone B4 was found to be derived from serum B. An almost identical HCV population was observed in the sample at day 9 p.i. In this sample, the dominant clone C1-1 and clone B4-1, which differs from clone B4 by only one amino acid, were detected. In contrast, more significant variation in quasispecies structure of the HCV species was observed in the sample at day 19 p.i. than that at day 9 p.i. With B4 as the dominant clone, the serum B-derived HCV species, clones B4 and B4-2, which differs from clone B4 by one amino acid, comprised 58% of the total population. Four types of HCV sequences derived from serum C were detected. Two of these (clones C1-3 and C1-4) contained lethal mutations. It was also found that the HCV species detected in the sample at day 33 p.i. included only two clones (clones B4 and B4-3), derived from serum B. The dominant clone, B4, was found to comprise 89% of the total population.

3.4. Potential use of the RFB system for evaluation of anti-HCV compounds

An experiment was carried out to determine whether this HCV infection experiment system was useful for the evaluation of anti-HCV drugs (Fig. 4). For this purpose, a small,

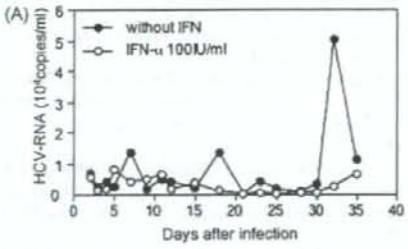

(B)

	Clone		(%)
Inocula	B4	KVLFVLLLFAGVDAETHVTGGSAGRTTAGLVSLLTPGAKQNIQLINTNGS	2.1
	C1	KVLIVHLLFAGVDGDTHVSGGTQGRAAVGLASLFALGPTQKIQLVNTNGS	13.9
Day 32	B4	----------	60
	B4-4	----------*----------	20
	C1-1	----------E-R-T--T--NV-ST-TSLF-P-AS----------	20

Fig. 4. A therapeutic effect of IFN in HCV infection model in the RFB cultures. HCV-infected FLC4 cells were treated with or without 100 IU/mL IFN-α. (A) Culture media were periodically collected, and HCV RNA levels were determined. Closed circles: without IFN treatment, open circles: treatment with IFN. (B) Changes in the viral quasispecies distribution in the cells without IFN treatment. Percentages in the inoculum or in the culture medium on day 32 p.i. are indicated at the right side. *, termination codon.

4-mL RFB column was adopted and a pair of RFB cultures infected with the HCV-positive pooled plasma (Table 1) was prepared. IFN-α was added to one culture at a final concentration of 100 IU/mL at 12 h p.i. No cytotoxicity was observed in FLC4 cells under these conditions (data not shown). Culture media from two cultures (12.5 mL each) were sampled periodically for 35 days and replaced by the same volume of fresh medium in the presence or absence of IFN-α. HCV RNA in the collected media was quantified by real-time RT-PCR, as described above. As shown in Fig. 4A, in the no-treatment culture, fluctuations in the viral RNA levels with the peaks on days 7, 18, and 32 p.i. ($1.5–5 \times 10^4$ copies/mL) were observed. However, while HCV RNA at $0.5–0.8 \times 10^4$ copies/mL was detected in the IFN-treated culture at days 5–11 p.i., no HCV RNA was detected at days 12–30 p.i. Serum levels of hepatic transaminases such as ALT and AST are known to be markers of liver damage. In the HCV-infection model with FLC4 cells cultured in RFB, the AST levels in the culture medium, which ranged from 5 to 10 IU/L without HCV infection, increased to 20–50 IU/L according to the viral infection (data not shown). Such increased AST levels were found to fall by the IFN treatment to lower than 10 IU/L at day 28 p.i. As reported previously, the ALT levels in the culture medium were constantly low; its levels were less than 10 IU/mL, with or without HCV infection (Aizaki et al., 2003). The viral nucleotide sequence in the no-treatment culture medium at day 32 p.i. was determined. It was found that serum B-derived clone B4 was dominant, and serum C-derived clone C1 was present as a minor clone (Fig. 4B); thus, the results corresponded well with those demonstrated in Fig. 3. An increase in viral RNA in the IFN-treated culture after day 32 p.i. was observed; although the degree of increase was only slight (Fig. 4A). It will be interesting to test whether HCV species grown in the IFN-treated culture is a variant resistant to IFN-α.

4. Discussion

At present an important limitation of the *in vitro* HCV infection system is that the only established culture system is based on genotype 2a, JFH-1 isolate, and Huh-7-derived cell lines. The development of alternate infection systems in which other HCV strains and host cells are available has been needed for the study of HCV dynamics and virus–host interactions, and for testing antivirals. This paper demonstrates that a long-term culture of the 3D RFB system is a useful tool for investigating HCV dynamics. The present results revealed that the viral quasispecies distribution altered in the HCV infection system in the RFB system. The change probably occurs in the following two-stage process. The first change was observed on day 3 p.i.; thus, it is possible that the HCV species were selected according to infectivity in FLC4 cells. It has been reported that HCV particle populations in chronic hepatitis C patients consist of low-density virions and higher-density immune complex forms (Hijikata et al., 1993; Kanto et al., 1994). Inoculation of cultured cells with HCV has demonstrated that the immune complex forms were less infective than the antibody-unbound virions (Shimizu et al., 1994). Therefore, another hypothesis may be that a large number of HCV populations in sera A, D, E, and F are immune complex forms; thus, these sera are less susceptible to the cells than sera B and C. The second change was observed on days 19–33 p.i. While the serum C-derived clone was dominant in the early stages after infection, the serum B-derived HCV clone became dominant over time. In the absence of immunological selection pressure, viral nucleotide mutations at random positions are accumulated during viral replication, and the newly generated variant species are selected principally, if not solely, based on the intrinsic replicative advantages or disadvantages that these mutations confer. Thus, these results suggest that the use of pooled serum sample allowed for screening of infectious materials compatible for the RFB culture.

Evaluation methods for anti-HCV drugs using monolayer culture systems with various culture cells, such as the replicon system and the JFH-1 based virion production system, have been reported (Bartenschlager et al., 2003; Blight et al., 2000; Boriskin et al., 2006; Lanford et al., 2003; Lindenbach et al., 2005; Lohmann et al., 1999; Wakita et al., 2005; Zhong et al., 2005). These methods utilize viral markers, such as HCV RNA and antigens, as indicators of treatment efficacy. However, the utility of long-term cell culture systems for anti-HCV drug evaluation based on infection with human sera is still limited. The use of a chimpanzee model, the only non-human host for HCV infection, is restricted due to several reasons such as problematic availability and ethical consideration. Given intensive efforts to reduce and replace animal testing in the course of development of new therapies worldwide, the RFB-based HCV infection model is a potential alternative to animal models such chimpanzee for assessing anti-HCV compounds. According to the studies with regards to mathematical modeling of HCV kinetics (Dahari et al., 2005; Dixit et al., 2004; Layden et al., 2003; Layden-Almer et al., 2006; Perelson et al., 2005), IFN therapy against HCV infection generally generates a biphasic decline in viral load; there is a rapid decrease in the serum HCV RNA level over the

first 1 day of treatment, followed by the second phase, which is slower than the first-phase viral decline. To date, there were no such observable viral kinetics in the IFN treatment under such experimental settings. Further detailed kinetic analyses of the use of varying doses of IFN and of very early time points to evaluate the antiviral effect are in progress.

In summary, by investigating the dynamics of HCV populations in the RFB culture system, it was demonstrated that HCV was intermittently detected in the culture supernatants of long-term culture, and that changes in viral quasispecies appear to be related to this fluctuation in the virus level. It was also shown that an HCV-infection model using the RFB system is useful for evaluating potential antivirals. Further investigation on the infection and growth of various HCV-positive sera is currently being conducted in order to obtain an adaptive clone with higher replication efficiency in this culture system.

Acknowledgements

The authors thank T. Wakita and S. Nagamori for helpful discussion and suggestions. We also thank M. Matsuda, T. Shimoji and M. Yahata for technical assistance, and T. Mizoguchi for secretarial work. This work was supported in part by a grant for Research on Health Sciences focusing on Drug Innovation from the Japan Health Sciences Foundation; by grants-in-aid from the Ministry of Health, Labor and Welfare; and by the program for Promotion of Fundamental Studies in Health Sciences of the National Institute of Biomedical Innovation, Japan.

References

Aizaki, H., Aoki, Y., Harada, T., Ishii, K., Suzuki, T., Nagamori, S., Toda, G., Matsuura, Y., Miyamura, T., 1998. Full-length complementary DNA of hepatitis C virus genome from an infectious blood sample. Hepatology 27, 621–627.

Aizaki, H., Nagamori, S., Matsuda, M., Kawakami, H., Hashimoto, O., Ishiko, H., Kawada, M., Matsuura, T., Hasumura, S., Matsuura, Y., Suzuki, T., Miyamura, T., 2003. Production and release of infectious hepatitis C virus from human liver cell cultures in the three-dimensional radial-flow bioreactor. Virology 314, 16–25.

Aoki, Y., Aizaki, H., Shimoike, T., Tani, H., Ishii, K., Saito, I., Matsuura, Y., Miyamura, T., 1998. A human liver cell line exhibits efficient translation of HCV RNAs produced by a recombinant adenovirus expressing T7 RNA polymerase. Virology 250, 140–150.

Bartenschlager, R., Kaul, A., Sparacio, S., 2003. Replication of the hepatitis C virus in cell culture. Antivir. Res. 60, 91–102.

Blight, K.J., Kolykhalov, A.A., Rice, C.M., 2000. Efficient initiation of HCV RNA replication in cell culture. Science 290, 1972–1974.

Boriskin, Y.S., Pecheur, E.I., Polyak, S.J., 2006. Arbidol: a broad-spectrum antiviral that inhibits acute and chronic HCV infection. Virol. J. 3, 56.

Choo, Q.L., Kuo, G., Weiner, A.J., Overby, L.R., Bradley, D.W., Houghton, M., 1989. Isolation of a cDNA clone derived from a blood-borne non-A, non-B viral hepatitis genome. Science 244, 359–362.

Choo, Q.L., Richman, K.H., Han, J.H., Berger, K., Lee, C., Dong, C., Gallegos, C., Coit, D., Medina-Selby, R., Barr, P.J., et al., 1991. Genetic organization and diversity of the hepatitis C virus. Proc. Natl. Acad. Sci. U.S.A. 88, 2451–2455.

Dahari, H., Major, M., Zhang, X., Mihalik, K., Rice, C.M., Perelson, A.S., Feinstone, S.M., Neumann, A.U., 2005. Mathematical modeling of primary hepatitis C infection: noncytolytic clearance and early blockage of virion production. Gastroenterology 128, 1056–1066.

Dixit, N.M., Layden-Almer, J.E., Layden, T.J., Perelson, A.S., 2004. Modelling how ribavirin improves interferon response rates in hepatitis C virus infection. Nature 432, 922–924.

Grakoui, A., McCourt, D.W., Wychowski, C., Feinstone, S.M., Rice, C.M., 1993. Characterization of the hepatitis C virus-encoded serine proteinase: determination of proteinase-dependent polyprotein cleavage sites. J. Virol. 67, 2832–2843.

Hijikata, M., Kato, N., Ootsuyama, Y., Nakagawa, M., Shimotohno, K., 1991. Gene mapping of the putative structural region of the hepatitis C virus genome by in vitro processing analysis. Proc. Natl. Acad. Sci. U.S.A. 88, 5547–5551.

Hijikata, M., Shimizu, Y.K., Kato, H., Iwamoto, A., Shih, J.W., Alter, H.J., Purcell, R.H., Yoshikura, H., 1993. Equilibrium centrifugation studies of hepatitis C virus: evidence for circulating immune complexes. J. Virol. 67, 1953–1958.

Hongo, T., Kajikawa, M., Ishida, S., Ozawa, S., Ohno, Y., Sawada, J., Umezawa, A., Ishikawa, Y., Kobayashi, T., Honda, H., 2005. Three-dimensional high-density culture of HepG2 cells in a 5-ml radial-flow bioreactor for construction of artificial liver. J. Biosci. Bioeng. 99, 237–244.

Ikeda, M., Sugiyama, K., Mizutani, T., Tanaka, T., Tanaka, K., Sekihara, H., Shimotohno, K., Kato, N., 1998. Human hepatocyte clonal cell lines that support persistent replication of hepatitis C virus. Virus Res. 56, 157–167.

Iwahori, T., Matsuura, T., Maehashi, H., Sugo, K., Saito, M., Hosokawa, M., Chiba, K., Masaki, T., Aizaki, H., Ohkawa, K., Suzuki, T., 2003. CYP3A4 inducible model for in vitro analysis of human drug metabolism using a bioartificial liver. Hepatology 37, 665–673.

Kanto, T., Hayashi, N., Takehara, T., Hagiwara, H., Mita, E., Naito, M., Kasahara, A., Fusamoto, H., Kamada, T., 1994. Buoyant density of hepatitis C virus recovered from infected hosts: two different features in sucrose equilibrium density-gradient centrifugation related to degree of liver inflammation. Hepatology 19, 296–302.

Kawada, M., Nagamori, S., Aizaki, H., Fukaya, K., Niiya, M., Matsuura, T., Sujino, H., Hasumura, S., Yashida, H., Mizutani, S., Ikenaga, H., 1998. Massive culture of human liver cancer cells in a newly developed radial flow bioreactor system: ultrafine structure of functionally enhanced hepatocarcinoma cell lines. In Vitro Cell Dev. Biol. Anim. 34, 109–115.

Kuo, G., Choo, Q.L., Alter, H.J., Gitnick, G.L., Redeker, A.G., Purcell, R.H., Miyamura, T., Dienstag, J.L., Alter, M.J., Stevens, C.E., et al., 1989. An assay for circulating antibodies to a major etiologic virus of human non-A, non-B hepatitis. Science 244, 362–364.

Lanford, R.E., Guerra, B., Lee, H., Averett, D.R., Pfeiffer, B., Chavez, D., Notvall, L., Bigger, C., 2003. Antiviral effect and virus-host interactions in response to alpha interferon, gamma interferon, poly(i)–poly(c), tumor necrosis factor alpha, and ribavirin in hepatitis C virus subgenomic replicons. J. Virol. 77, 1092–1104.

Layden, T.J., Layden, J.E., Ribeiro, R.M., Perelson, A.S., 2003. Mathematical modeling of viral kinetics: a tool to understand and optimize therapy. Clin. Liver Dis. 7, 163–178.

Layden-Almer, J.E., Cotler, S.J., Layden, T.J., 2006. Viral kinetics in the treatment of chronic hepatitis C. J. Viral Hepat. 13, 499–504.

Lindenbach, B.D., Evans, M.J., Syder, A.J., Wolk, B., Tellinghuisen, T.L., Liu, C.C., Maruyama, T., Hynes, R.O., Burton, D.R., McKeating, J.A., Rice, C.M., 2005. Complete replication of hepatitis C virus in cell culture. Science 309, 623–626.

Lohmann, V., Korner, F., Koch, J., Herian, U., Theilmann, L., Bartenschlager, R., 1999. Replication of subgenomic hepatitis C virus RNAs in a hepatoma cell line. Science 285, 110–113.

Martell, M., Esteban, J.I., Quer, J., Genesca, J., Weiner, A., Esteban, R., Guardia, J., Gomez, J., 1992. Hepatitis C virus (HCV) circulates as a population of different but closely related genomes: quasispecies nature of HCV genome distribution. J. Virol. 66, 3225–3229.

Murakami, K., Ishii, K., Ishihara, Y., Yoshizaki, S., Tanaka, K., Gotoh, Y., Aizaki, H., Kohara, M., Yoshioka, H., Mori, Y., Manabe, N., Shoji, I., Sata, T., Bartenschlager, R., Matsuura, Y., Miyamura, T., Suzuki, T., 2006. Production of infectious hepatitis C virus particles in three-dimensional cultures of the cell line carrying the genome-length dicistronic viral RNA of genotype 1b. Virology 351, 381–392.

Pawlotsky, J.M., 2006. Hepatitis C virus population dynamics during infection. Curr. Top. Microbiol. Immunol. 299, 261–284.

Perelson, A.S., Herrmann, E., Micol, F., Zeuzem, S., 2005. New kinetic models for the hepatitis C virus. Hepatology 42, 749–754.

Poynard, T., Yuen, M.F., Ratziu, V., Lai, C.L., 2003. Viral hepatitis C. Lancet 362, 2095–2100.

Saito, I., Miyamura, T., Ohbayashi, A., Harada, H., Katayama, T., Kikuchi, S., Watanabe, Y., Koi, S., Onji, M., Ohta, Y., et al., 1990. Hepatitis C virus infection is associated with the development of hepatocellular carcinoma. Proc. Natl. Acad. Sci. U.S.A. 87, 6547–6549.

Shimizu, Y.K., Hijikata, M., Iwamoto, A., Alter, H.J., Purcell, R.H., Yoshikura, H., 1994. Neutralizing antibodies against hepatitis C virus and the emergence of neutralization escape mutant viruses. J. Virol. 68, 1494–1500.

Suzuki, T., Omata, K., Satoh, T., Miyasaka, T., Arai, C., Maeda, M., Matsuno, T., Miyamura, T., 2005. Quantitative detection of hepatitis C virus (HCV) RNA in saliva and gingival crevicular fluid of HCV-infected patients. J. Clin. Microbiol. 43, 4413–4417.

Tagawa, M., Kato, N., Yokosuka, O., Ishikawa, T., Ohto, M., Omata, M., 1995. Infection of human hepatocyte cell lines with hepatitis C virus in vitro. J. Gastroenterol. Hepatol. 10, 523–527.

Wakita, T., Pietschmann, T., Kato, T., Date, T., Miyamoto, M., Zhao, Z., Murthy, K., Habermann, A., Krausslich, H.G., Mizokami, M., Bartenschlager, R., Liang, T.J., 2005. Production of infectious hepatitis C virus in tissue culture from a cloned viral genome. Nat. Med. 11, 791–796.

Zhong, J., Gastaminza, P., Cheng, G., Kapadia, S., Kato, T., Burton, D.R., Wieland, S.F., Uprichard, S.L., Wakita, T., Chisari, F.V., 2005. Robust hepatitis C virus infection in vitro. Proc. Natl. Acad. Sci. U.S.A. 102, 9294–9299.

Journal of General Virology (2008), 89, 1587–1592 DOI 10.1099/vir.0.83618-0

Short Communication

Virological characterization of the hepatitis C virus JFH-1 strain in lymphocytic cell lines

Kyoko Murakami,[1] Toshiro Kimura,[1] Motonao Osaki,[1] Koji Ishii,[1] Tatsuo Miyamura,[1] Tetsuro Suzuki,[1] Takaji Wakita[1] and Ikuo Shoji[1,2]

Correspondence
Ikuo Shoji
ishoji@med.kobe-u.ac.jp

[1]Department of Virology II, National Institute of Infectious Diseases, 1-23-1 Toyama, Shinjuku-ku, Tokyo 162-8640, Japan

[2]Division of Microbiology, Kobe University Graduate School of Medicine, 7-5-1 Kusunoki-cho, Chuo-ku, Kobe, Hyogo 650-0017, Japan

While hepatocytes are the major site of hepatitis C virus (HCV) infection, a number of studies have suggested that HCV can replicate in lymphocytes. However, *in vitro* culture systems to investigate replication of HCV in lymphocytic cells are severely limited. Robust HCV culture systems have been established using the HCV JFH-1 strain and Huh-7 cells. To gain more insights into the tissue tropism of HCV, we investigated the infection, replication, internal ribosome entry site (IRES)-dependent translation and polyprotein processing of the HCV JFH-1 strain in nine lymphocytic cell lines. HCV JFH-1 failed to infect lymphocytes and replicate, but exhibited efficient polyprotein processing and IRES-dependent translation in lymphocytes as well as in Huh-7 cells. Our results suggest that lymphocytic cells can support HCV JFH-1 translation and polyprotein processing, but may lack some host factors essential for HCV JFH-1 infection and replication.

Received 25 November 2007
Accepted 18 March 2008

Hepatitis C virus (HCV) is a major cause of chronic hepatitis, liver cirrhosis and hepatocellular carcinoma (Choo *et al.*, 1989; Saito *et al.*, 1990). Infection with HCV is frequently associated with B-cell-related diseases, such as mixed cryoglobulinaemia and non-Hodgkin's lymphoma (Hausfater *et al.*, 2000). A number of studies have suggested that HCV can replicate not only in hepatocytes, but also in lymphocytes (Ducoulombier *et al.*, 2004; Karavattathayyil *et al.*, 2000, Lerat *et al.*, 1998), whereas the determinants of HCV tropism are still unknown. The development of HCV strain JFH-1, which generates infectious HCV in culture, has made an important contribution to the study of the HCV life cycle (Lindenbach *et al.*, 2005; Wakita *et al.*, 2005; Zhong *et al.*, 2005). The HCV life cycle is divided into several steps. After entry into the cell and uncoating, the HCV life cycle leads to translation, polyprotein processing, RNA replication, virion assembly, transport and release. The JFH-1 subgenomic replicon can replicate in non-hepatic cell lines, such as HeLa cells and 293 cells, suggesting that the host factors required for HCV replication are not hepatocyte-specific (Kato *et al.*, 2005b). The SB strain of HCV (genotype 2b strain) was isolated from an HCV-infected non-Hodgkin's B-cell lymphoma and has been reported to infect B and T cells (Kondo *et al.*, 2007; Sung *et al.*, 2003). The virus titres of the SB strain in lymphocytes were, however, lower than those of JFH-1 in Huh-7 cells and the expression of HCV proteins was not confirmed (Kondo *et al.*, 2007). It is unknown whether HCV JFH-1 can infect and replicate in lymphocytes. To gain more insight into the tissue tropism of HCV infection, we investigated the infection, replication, IRES-dependent translation and polyprotein processing of the JFH-1 strain in nine lymphocytic cell lines.

We first sought to determine whether HCV JFH-1 can infect lymphocytic cell lines. We chose nine lymphocytic cell lines derived from Burkitt's lymphoma, the EBV-immortalized human B cell line, lymphoblasts and acute T-cell leukaemia. C1R, IB4, Namalwa, P3HR1 and Raji cells were Epstein–Barr virus (EBV)-positive (Table 1). Infectious HCV was generated from HCV JFH-1 RNA in Huh-7 cells (Shirakura *et al.*, 2007; Wakita *et al.*, 2005) and the calculation of the 50 % tissue culture infectious dose ($TCID_{50}$) was based on methods described previously (Lindenbach *et al.*, 2005). These cell lines (1×10^5 cells per well of a six-well plate) were incubated with 2 ml inoculum (5×10^3 or 5×10^4 $TCID_{50}$ ml^{-1}) for 3 h, washed three times with PBS, and cultured in fresh medium. The culture medium was changed every 2 days. Cells were harvested at 0 (3 h post-infection [p.i.]), 4 and 8 day p.i. HCV core antigen within cells was quantified by immunoassay (Ortho HCV-core ELISA kit; Ortho-Clinical Diagnostics). As shown in Fig. 1(a), increasing the HCV titre of the inoculum resulted in a 7.2-fold increase in the levels of HCV core protein in Huh-7 cells at 3 h p.i. Increasing the HCV titre of the inoculum resulted in a 1.5- to 3.2-fold increase in the levels of the core protein in C1R, BL41,

Table 1. Summary of the virological characterization of HCV JFH-1 in lymphocytes

Name	Source	EBV	Transfection			Concentration of G418 for selection (μg ml^{-1})	HCVcc infection	HCV-RNA replication	Translation*		Polyprotein processing†
			Buffer	Program	Efficiency				HCV-IRES	EMCV-IRES	
Bjab	Burkitt's lymphoma	–	T	T–16	>90 %	600–800	–	–	+	+ +	+
BL41	Burkitt's lymphoma	–	V	I–10	60–70 %	1000	–	–	+	+ +	ND
C1R	B lymphoblast	+	V	T–20	70–80 %	100	–	–	+ + +	+ + + +	+
IB4	Lymphoblastoid	+	V	T–20	80–90 %	1000	–	–	+ + +	+ + + +	+
Jurkat	Acute T cell leukaemia	–	V	I–10	60–70 %	600	–	–	+ +	+	ND
Namalwa	Burkitt's lymphoma	+	V	M–13	60–70 %	600–800	–	–	+ + +	+ + + +	+
P3HR1	Burkitt's lymphoma	+	V	A–23	60–70 %	800	–	–	+ + +	+ + + +	ND
Raji	Burkitt's lymphoma	+	V	T–27	70–80 %	800	–	–	+ +	+ + + +	+
Ramos	Burkitt's lymphoma	–	V	M–13	40–60 %	400	–	–	+	+	ND
Huh7	Hepatoma	–	T	T–14	70–80 %	500	+	+	+ + +	+ + +	+

*+, <0.25 fold IRES activity of Huh-7; + +, 0.25–0.75 fold; + + +, 0.75–1.5-fold; + + + +, >1.5-fold.
†ND, Not determined.

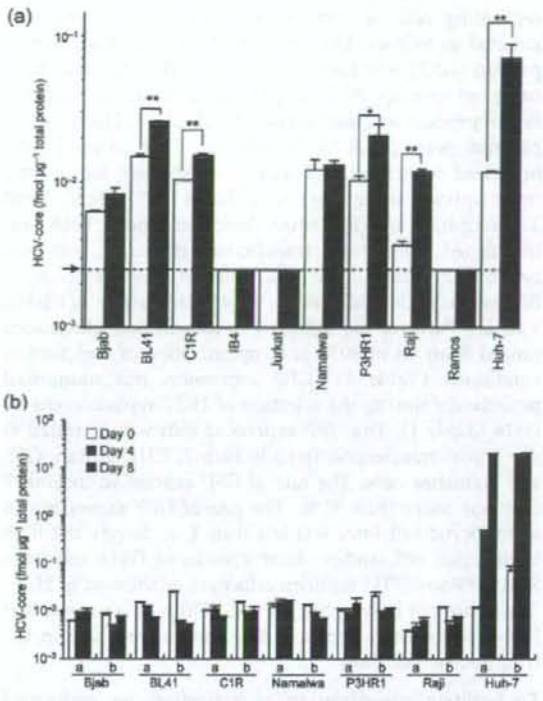

Fig. 1. HCV infection assay. (a) HCV core protein levels 3 h after infection. A total of 1×10^5 cells were infected with 2 ml of the inoculum (5×10^3 [white bars] or 5×10^4 [grey bars] $TCID_{50}$ ml^{-1}) for 3 h at 37 °C and harvested at 3 h p.i. HCV core protein in cell lysate was quantified by ELISA. The average values with standard deviations from triplicate samples are shown. The cut-off value of the immunoassay is indicated by an arrow and a dotted line. The difference between low m.o.i. (white bars) and high m.o.i. (grey bars) was significant (*, $P<0.05$; **, $P<0.01$, Student's *t*-test). (b) Time-course of HCV core protein levels after infection. In total, 1×10^5 cells were infected with 2 ml of the inoculum (5×10^3 [a] or 5×10^4 [b] $TCID_{50}$ ml^{-1}) for 3 h and harvested at 0, 4 and 8 days p.i. HCV core protein in cell lysate was quantified by ELISA. Average values ± SD from triplicate samples are shown.

P3HR1 and Raji cells, suggesting that HCV can bind to these cell lines (Fig. 1a). In contrast, the levels of HCV core protein in IB4, Jurkat and Ramos cells at 3 h p.i. were below the detection limits and there were no significant differences in the levels of the core protein in Bjab cells and Namalwa cells, suggesting that HCV binding to these cells was very inefficient (Fig. 1a). Moreover, the levels of HCV core protein increased in Huh-7 cells but, in the case of all lymphocytic cell lines, including Raji cells, the core titre did not increase at day 4 and 8 p.i., suggesting that HCV JFH-1 does not infect and/or replicate efficiently in these lymphocytic cell lines (Fig. 1b).

To assess the replication of JFH-1 in our lymphocytic cell lines, we utilized the HCV replicon system. To visualize the

replicating cells, a reporter replicon plasmid was constructed as follows. The gene encoding green fluorescence protein (GFP) was fused to the neomycin resistance gene using an overlap PCR amplification technique and the fusion product was inserted into pSGR-JFH1. The resultant plasmid was pSGR-GFPneo-JFH1. This plasmid was linearized with *Xba*I and used as a template for *in vitro* transcription using an AmpliScribe T7 High Yield Transcription kit (Epicentre Biotechnologies). RNA was transfected with high transfection efficiency and low cytotoxicity using the Nucleofector system (Amaxa Biosystems) (Coughlin *et al.*, 2004; Miyahara *et al.*, 2005; Van De Parre *et al.*, 2005). The transfection efficiencies ranged from 60 to 80 % after optimization of transfection conditions (Table 1). GFP expression was monitored periodically during the selection of HCV-replicon cells by G418 (Table 1). The GFP-expressing cells were detected at day 3 post-transfection (p.t.) in Huh-7, P3HR1, Raji, C1R and Namalwa cells. The rate of GFP expression in Huh-7 cells was more than 50 %. The rate of GFP-expression in lymphocytic cell lines was less than 1 %, despite the high transfection efficiencies. After 3 weeks of G418 selection, SGR-GFPneo-JFH1 replicon cells were established in Huh-7 cells, but not in lymphocytic cells. These data suggest that JFH-1 subgenomic replicon RNA cannot replicate in the lymphocytic cell lines.

To facilitate quantification of replication, we performed luciferase assays using subgenomic replicon RNA (SGR-JFH1/Luc) carrying firefly luciferase as a reporter. SGR-JFH1/Luc RNA was *in vitro*-transcribed using the linearized pSGR-JFH1/Luc (Kato *et al.*, 2005a) as template DNA. Cells were harvested at 4, 24, 48 and 72 h p.t. and luciferase activities were assayed with luciferase assay reagent (Promega). Assays were performed at least in triplicate. There were significant differences in luciferase activities at 4 h p.t. among the cell lines, probably because there were differences in transfection efficiencies and the doubling time of the cell lines. Thus, the replication activity was expressed relative to the reporter activity determined 4 h p.t. for each cell line, which was set to 1 (Fig. 2a). HCV subgenomic replicon RNA efficiently replicated in Huh-7 cells (Fig. 2a). Replication-deficient subgenomic replicon RNA encoding a GDD to GND mutation in NS5B served as a negative control in Huh-7 cells. The luciferase activities of replication-deficient subgenomic replicon RNA in lymphocytic cell lines also decreased rapidly (data not shown). As shown in Fig. 2(a), the luciferase activities of HCV subgenomic replicon RNA in lymphocytic cell lines decreased rapidly, suggesting that HCV subgenomic replicon RNA did not replicate efficiently in lymphocytic cell lines. Thus, these two different replicon assays demonstrated that the HCV JFH-1 subgenomic replicon failed to replicate in our lymphocytic cell lines.

To determine which steps of the HCV life cycle are impaired, we further examined translation and polyprotein processing. At first, we assessed HCV IRES-dependent translational efficiencies in the lymphocytic cell lines. Cells were co-transfected with the subgenomic replicon RNA (SGR-JFH1/Luc) and a capped RNA encoding *Renilla* luciferase (cap-luc). Cap-luc RNA was *in vitro*-transcribed using a T7 mMessage mMachine kit (Ambion). The HCV IRES activities in IB4, Namalwa and P3HR1 cells were as high as in Huh-7 cells. The HCV IRES activities in Jurkat and Raji cells were about 50 % of those in Huh-7 cells, and the HCV IRES activities in Bjab, BL41 and Ramos cells were less than 25 % of those in Huh-7 cells. On the other hand, the HCV IRES activity in C1R cells was about twofold higher than in Huh-7 cells (Fig. 2b). Replication-deficient subgenomic replicon RNA encoding a GDD to GND mutation in NS5B showed a luciferase activity level similar to that of the wild-type, suggesting that the luciferase activity at 4 h after transfection reflected translational levels but not replication levels (data not shown). Our data indicate high HCV IRES activities in all cell lines, except in Bjab, BL41 and Ramos.

The HCV polyprotein is translated in subgenomic replicon cells in an encephalomyocarditis virus (EMCV) IRES-dependent manner. To rule out the possibility that the EMCV IRES-dependent translation is impaired in lymphocytic cell lines, we assessed the EMCV IRES-dependent translational efficiencies. We assayed EMCV IRES activity using EMCV IRES-driven luciferase RNA (EMC-luc) and Cap-luc RNA. The EMCV IRES activity was five- to tenfold higher in C1R, Namalwa, IB4 and P3HR1 than in Huh-7 cells (Fig. 2c). From these results, HCV IRES and EMCV IRES exhibited sufficient translational activity in C1R, Namalwa, P3HR1 and Raji cells, suggesting that IRES-dependent translation was not impaired in these lymphocytic cell lines.

To determine whether HCV polyprotein is properly processed in lymphocytes, we examined the processing of HCV non-structural (NS) proteins. The construct pSGR-JFH1/Luc expresses the polyprotein NS3-NS4A-NS4B-NS5A-NS5B. The HCV NS3/4A protease is responsible for proteolytic processing at each cleavage site. We used the eukaryotic transient-expression system based on a recombinant vaccinia virus carrying bacteriophage T7 RNA polymerase (T7vac) (Fuerst *et al.*, 1989). To express the SGR-JFH1/Luc encoding HCV NS proteins, 5×10^6 cells were transfected with 5 μg pSGR-JFH1/Luc and infected with 2.5×10^9 p.f.u. T7vac, harvested at 24 h p.i., and analysed by Western blotting. Completely processed NS3, NS5A and NS5B proteins were detected in Bjab, Raji, IB4 and Namalwa cells as well as in pSGR-JFH1/Luc-transfected Huh-7 cells and HCV-JFH1-infected Huh-7 cells (Fig. 2c). The unprocessed polyprotein was not detected by immunoblotting in these lymphocytic cell lines (data not shown). These results suggest that the HCV polyprotein is efficiently processed in these lymphocytic cells.

In this study, we demonstrated that HCV JFH-1 failed to infect and replicate in nine lymphocytic cell lines. In contrast, HCV IRES-dependent translation and polyprotein processing by NS3/NS4A protease functioned properly

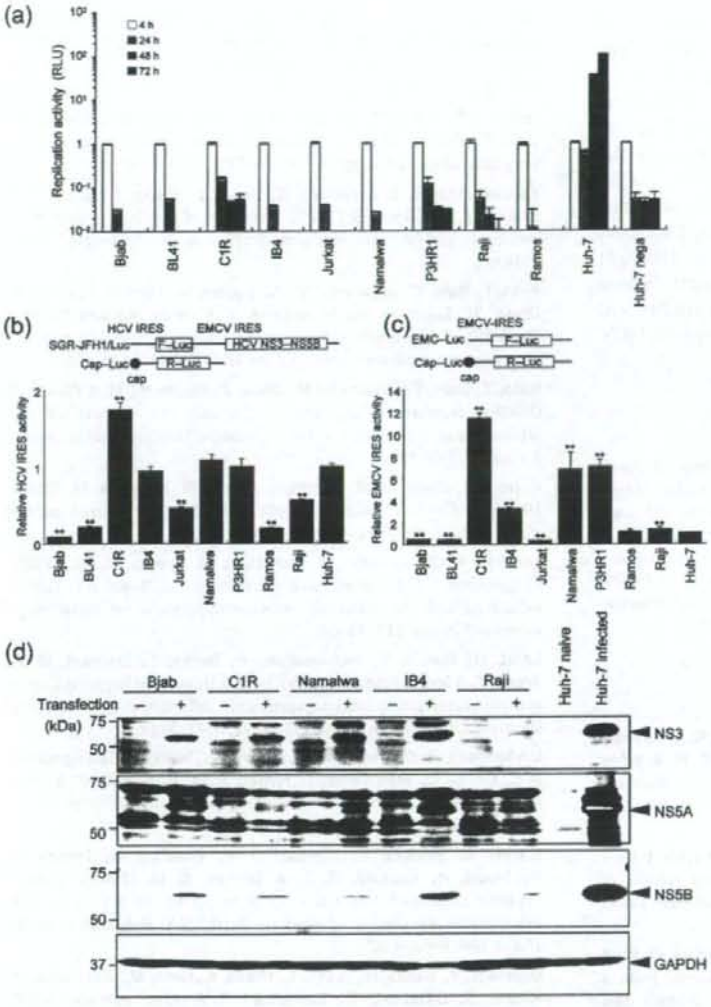

Fig. 2. Replication, HCV IRES-dependent translational efficiencies and polyprotein processing. (a) Subgenomic replicon assay. JFH-1 subgenomic replicon RNA was transfected into several cell lines and harvested at 4, 24, 48 and 72 h p.t. The replication activity was expressed relative to the reporter activity determined 4 h p.t. for each cell line, which was set to 1. RLU, Relative luciferase units; Huh-7 nega, Huh-7 cells transfected with SGR-JFH1/Luc GND, served as a negative control. (b) HCV IRES-dependent translational efficiency. To determine the HCV IRES activities, we co-transfected cells with SGR-JFH1/Luc RNA and Cap-Renilla luciferase RNA. The IRES activity of each cell line is expressed in relation to Huh-7 IRES activity, that is, as the ratio of HCV IRES-driven firefly luciferase activity to cap-driven *Renilla* luciferase activity. The difference in HCV IRES activity between Huh-7 cells and the lymphocytic cell line was significant (**, $P<0.01$, Student's *t*-test). (c) EMCV IRES-dependent translational efficiency. To determine the EMCV IRES activities, we co-transfected cells with EMCV–firefly luciferase RNA and Cap-Renilla luciferase RNA. The IRES activity of each cell line is expressed in relation to Huh-7 IRES activity, that is, as the ratio of EMCV IRES-driven firefly luciferase activity to cap-driven *Renilla* luciferase activity. The difference in EMCV IRES activity between Huh-7 cell and the lymphocytic cell line was significant (**, $P<0.01$, Student's *t*-test). (d) Polyprotein processing by NS3/4A protease in lymphocytic cell lines. pSGR-JFH1/Luc-transfected cells were infected with T7vac and harvested at 24 h p.i. HCV NS proteins, NS3, NS5A and NS5B were detected by using anti-NS3 rabbit polyclonal antibody (PAb), anti-NS5A rabbit PAb and anti-NS5B rabbit PAb. Arrowheads indicate the processed NS3, NS5A and NS5B proteins, respectively.

in these cells. Moreover, subgenomic replicon RNA failed to replicate in these cell lines. Our data suggest that lymphocytic cell lines may lack some host factors required for infection and replication of HCV-JFH1.

Viral entry often requires sequential interactions between viral proteins and several cellular factors. Several molecules (CD81, Claudin-1, Scavenger receptor class B member IR, LDL-receptor and glycosaminoglycans) have been reported to be involved in HCV binding and entry (Barth *et al.*, 2003; Evans *et al.*, 2007; Pileri *et al.*, 1998; Scarselli *et al.*, 2002). Further investigation will be required to clarify HCV binding and entry into lymphocytic cell lines.

HCV IRES and EMCV IRES exhibited sufficient translational activities in C1R, IB4, P3HR1, Namalwa and Raji cells. All these cell lines are EBV-positive. EBV-encoded nuclear antigen (EBNA1) has been reported to support HCV replication (Sugawara *et al.*, 1999). Two small EBV-encoded RNA species (EBERs) bind to the HCV IRES region (Wood *et al.*, 2001). These findings raise the possibility that HCV IRES activities may be modified by the EBV genome.

HCV JFH-1 subgenomic replicon RNA could not replicate in all lymphocytes tested in this study. The HCV SB strain, however, has been reported to infect Raji, Daudi, Molt-4

and Jurkat cells (Kondo *et al.*, 2007; Sung *et al.*, 2003). Still unknown is how hepatotropism and lymphotropism of HCV are determined. The GB virus B (GBV-B) is most closely related to HCV and the GBV-B infection of tamarins has been proposed as a good surrogate model for chronic hepatitis C (Bukh *et al.*, 2001; Jacob *et al.*, 2004; Lanford *et al.*, 2003; Martin *et al.*, 2003). A recent report has shown that GBV can disseminate to not only liver but also a variety of extrahepatic tissues such as haematolymphoid and genital tissues in tamarins (Ishii *et al.*, 2007). Viral RNA cloned from plasma and liver from the tamarins showed no sequence heterogeneity, suggesting that host factors determine the pleiotropism (Ishii *et al.*, 2007). It remains unclear how host factors and/or viral factors determine the tissue tropism of HCV. Further studies will be required to clarify the molecular mechanisms of HCV tissue tropism.

Acknowledgements

The authors gratefully acknowledge Drs Sanae Machida (Saitama Medical School, Saitama, Japan), Shizuko Harada (NIID, Tokyo, Japan) and Isao Hamaguchi (NIID, Tokyo, Japan) for the cell lines, and Dr Hideki Aizaki (NIID, Tokyo, Japan) for helpful discussion. This work was supported in part by grants-in-aid from the Ministry of Health, Labour and Welfare, by a grant for Research on Health Sciences focusing on Drug Innovation from the Japan Health Sciences Foundation, and by grant-in aid for young scientists (B).

References

Barth, H., Schafer, C., Adah, M. I., Zhang, F., Linhardt, R. J., Toyoda, H., Kinoshita-Toyoda, A., Toida, T., Van Kuppevelt, T. H. & other authors (2003). Cellular binding of hepatitis C virus envelope glycoprotein E2 requires cell surface heparan sulfate. *J Biol Chem* **278**, 41003–41012.

Bukh, J., Apgar, C. L., Govindarajan, S. & Purcell, R. H. (2001). Host range studies of GB virus-B hepatitis agent, the closest relative of hepatitis C virus, in New World monkeys and chimpanzees. *J Med Virol* **65**, 694–697.

Choo, Q. L., Kuo, G., Weiner, A. J., Overby, L. R., Bradley, D. W. & Houghton, M. (1989). Isolation of a cDNA clone derived from a blood-borne non-A, non-B viral hepatitis genome. *Science* **244**, 359–362.

Coughlin, C. M., Vance, B. A., Grupp, S. A. & Vonderheide, R. H. (2004). RNA-transfected CD40-activated B cells induce functional T-cell responses against viral and tumor antigen targets: implications for pediatric immunotherapy. *Blood* **103**, 2046–2054.

Ducoulombier, D., Roque-Afonso, A. M., Di Liberto, G., Penin, F., Kara, R., Richard, Y., Dussaix, E. & Feray, C. (2004). Frequent compartmentalization of hepatitis C virus variants in circulating B cells and monocytes. *Hepatology* **39**, 817–825.

Evans, M. J., von Hahn, T., Tscherne, D. M., Syder, A. J., Panis, M., Wolk, B., Hatziioannou, T., McKeating, J. A., Bieniasz, P. D. & Rice, C. M. (2007). Claudin-1 is a hepatitis C virus co-receptor required for a late step in entry. *Nature* **446**, 801–805.

Fuerst, T. R., Fernandez, M. P. & Moss, B. (1989). Transfer of the inducible *lac* repressor/operator system from *Escherichia coli* to a vaccinia virus expression vector. *Proc Natl Acad Sci U S A* **86**, 2549–2553.

Hausfater, P., Rosenthal, E. & Cacoub, P. (2000). Lymphoproliferative diseases and hepatitis C virus infection. *Ann Med Interne (Paris)* **151**, 53–57.

Ishii, K., Iijima, S., Kimura, N., Lee, Y. J., Ageyama, N., Yagi, S., Yamaguchi, K., Maki, N., Mori, K. & other authors (2007). GBV-B as a pleiotropic virus: distribution of GBV-B in extrahepatic tissues *in vivo*. *Microbes Infect* **9**, 515–521.

Jacob, J. R., Lin, K. C., Tennant, B. C. & Mansfield, K. G. (2004). GB virus B infection of the common marmoset (*Callithrix jacchus*) and associated liver pathology. *J Gen Virol* **85**, 2525–2533.

Karavattathayyil, S. J., Kalkeri, G., Liu, H. J., Gaglio, P., Garry, R. F., Krause, J. R. & Dash, S. (2000). Detection of hepatitis C virus RNA sequences in B-cell non-Hodgkin lymphoma. *Am J Clin Pathol* **113**, 391–398.

Kato, T., Date, T., Miyamoto, M., Sugiyama, M., Tanaka, Y., Orito, E., Ohno, T., Sugihara, K., Hasegawa, I. & other authors (2005a). Detection of anti-hepatitis C virus effects of interferon and ribavirin by a sensitive replicon system. *J Clin Microbiol* **43**, 5679–5684.

Kato, T., Date, T., Miyamoto, M., Zhao, Z., Mizokami, M. & Wakita, T. (2005b). Nonhepatic cell lines HeLa and 293 support efficient replication of the hepatitis C virus genotype 2a subgenomic replicon. *J Virol* **79**, 592–596.

Kondo, Y., Sung, V. M., Machida, K., Liu, M. & Lai, M. M. (2007). Hepatitis C virus infects T cells and affects interferon-gamma signaling in T cell lines. *Virology* **361**, 161–173.

Lanford, R. E., Chavez, D., Notvall, L. & Brasky, K. M. (2003). Comparison of tamarins and marmosets as hosts for GBV-B infections and the effect of immunosuppression on duration of viremia. *Virology* **311**, 72–80.

Lerat, H., Rumin, S., Habersetzer, F., Berby, F., Trabaud, M. A., Trepo, C. & Inchauspe, G. (1998). In vivo tropism of hepatitis C virus genomic sequences in hematopoietic cells: influence of viral load, viral genotype, and cell phenotype. *Blood* **91**, 3841–3849.

Lindenbach, B. D., Evans, M. J., Syder, A. J., Wolk, B., Tellinghuisen, T. L., Liu, C. C., Maruyama, T., Hynes, R. O., Burton, D. R. & other authors (2005). Complete replication of hepatitis C virus in cell culture. *Science* **309**, 623–626.

Martin, A., Bodola, F., Sangar, D. V., Goettge, K., Popov, V., Rijnbrand, R., Lanford, R. E. & Lemon, S. M. (2003). Chronic hepatitis associated with GB virus B persistence in a tamarin after intrahepatic inoculation of synthetic viral RNA. *Proc Natl Acad Sci U S A* **100**, 9962–9967.

Miyahara, Y., Naota, H., Wang, L., Hiasa, A., Goto, M., Watanabe, M., Kitano, S., Okumura, S., Takemitsu, T. & other authors (2005). Determination of cellularly processed HLA-A2402-restricted novel CTL epitopes derived from two cancer germ line genes, MAGE-A4 and SAGE. *Clin Cancer Res* **11**, 5581–5589.

Pileri, P., Uematsu, Y., Campagnoli, S., Galli, G., Falugi, F., Petracca, R., Weiner, A. J., Houghton, M., Rosa, D. & other authors (1998). Binding of hepatitis C virus to CD81. *Science* **282**, 938–941.

Saito, I., Miyamura, T., Ohbayashi, A., Harada, H., Katayama, T., Kikuchi, S., Watanabe, Y., Koi, S., Onji, M. & other authors (1990). Hepatitis C virus infection is associated with the development of hepatocellular carcinoma. *Proc Natl Acad Sci U S A* **87**, 6547–6549.

Scarselli, E., Ansuini, H., Cerino, R., Roccasecca, R. M., Acali, S., Filocamo, G., Traboni, C., Nicosia, A., Cortese, R. & Vitelli, A. (2002). The human scavenger receptor class B type I is a novel candidate receptor for the hepatitis C virus. *EMBO J* **21**, 5017–5025.

Shirakura, M., Murakami, K., Ichimura, T., Suzuki, R., Shimoji, T., Fukuda, K., Abe, K., Sato, S., Fukasawa, M. & other authors (2007).

E6AP ubiquitin ligase mediates ubiquitylation and degradation of hepatitis C virus core protein. *J Virol* **81**, 1174–1185.

Sugawara, Y., Makuuchi, M., Kato, N., Shimotohno, K. & Takada, K. (1999). Enhancement of hepatitis C virus replication by Epstein–Barr virus-encoded nuclear antigen 1. *EMBO J* **18**, 5755–5760.

Sung, V. M., Shimodaira, S., Doughty, A. L., Picchio, G. R., Can, H., Yen, T. S., Lindsay, K. L., Levine, A. M. & Lai, M. M. (2003). Establishment of B-cell lymphoma cell lines persistently infected with hepatitis C virus in vivo and in vitro: the apoptotic effects of virus infection. *J Virol* **77**, 2134–2146.

Van De Parre, T. J., Martinet, W., Schrijvers, D. M., Herman, A. G. & De Meyer, G. R. (2005). mRNA but not plasmid DNA is efficiently transfected in murine J774A.1 macrophages. *Biochem Biophys Res Commun* **327**, 356–360.

Wakita, T., Pietschmann, T., Kato, T., Date, T., Miyamoto, M., Zhao, Z., Murthy, K., Habermann, A., Krausslich, H. G. & other authors (2005). Production of infectious hepatitis C virus in tissue culture from a cloned viral genome. *Nat Med* **11**, 791–796.

Wood, J., Frederickson, R. M., Fields, S. & Patel, A. H. (2001). Hepatitis C virus 3′X region interacts with human ribosomal proteins. *J Virol* **75**, 1348–1358.

Zhong, J., Gastaminza, P., Cheng, G., Kapadia, S., Kato, T., Burton, D. R., Wieland, S. F., Uprichard, S. L., Wakita, T. & Chisari, F. V. (2005). Robust hepatitis C virus infection *in vitro*. *Proc Natl Acad Sci U S A* **102**, 9294–9299.

Treatment of Chronic Hepatitis C

Intervirology

Intervirology 2008;51(suppl 1):70–75
DOI: 10.1159/000122601

Published online: June 10, 2008

Usefulness of a New Immunoradiometric Assay of HCV Core Antigen to Predict Virological Response during PEG-IFN/RBV Combination Therapy for Chronic Hepatitis with High Viral Load of Serum HCV RNA Genotype 1b

Noriko Sasase[a] Soo Ryang Kim[b] Ke Ih Kim[a] Miyuki Taniguchi[b] Susumu Imoto[b] Keiji Mita[b] Hak Hotta[c] Ikuo Shouji[c] Ahmed El-Shamy[c] Norifumi Kawada[e] Masatoshi Kudo[f] Yoshitake Hayashi[d]

Departments of [a]Pharmacy and [b]Gastroenterology, Kobe Asahi Hospital, [c]Division of Microbiology, Kobe University Graduate School of Medicine, and [d]Division of Molecular Medicine and Medical Genetics, International Center for Medical Research and Treatment, Kobe University Graduate School of Medicine, Kobe, [e]Department of Hepatology, Osaka City University Medical School, Osaka, and [f]Department of Gastroenterology, Kinki University School of Medicine, Osakasayama, Japan

Key Words

Chronic hepatitis · HCV core antigen · HCV RNA genotype 1b · Immunoradiometric assay · PEG-IFN/RBV combination therapy · Prediction, virological response

Abstract

We investigated the clinical usefulness of a new immunoradiometric (IRM) assay of hepatitis C virus (HCV) core antigen in predicting virological response during pegylated interferon plus ribavirin (PEG-IFN/RBV) combination therapy for chronic hepatitis with high viral loads of serum HCV RNA genotype 1b. Thirty-nine patients received a regimen of PEG-IFNα-2b (1.5 μg/kg/week s.c.) in combination with RBV (600–1,000 mg/day). Of the 39 patients, 18 (46.2%) achieved sustained virological response (SVR), 11 (28.2%) attained partial response (PR) and 10 (25.6%) showed no response (NR). Four weeks after the start of therapy, 1- and 2-log reductions in the amount of HCV core antigen were observed in 20 (2/10) and 0% (0/10) showing NR, 91 (10/11) and 63.6% (7/11) with PRs, and 88.9 (16/18) and 55.6% (10/18) of patients with SVR, respectively. The 1- and 2-log reductions 4 weeks after the start of therapy were not a defining condition for PR and SVR. The amount of HCV core antigen was significantly different between SVR and PR patients on days 1 and 7, and between patients with NR and SVR at all points of time. In conclusion, this new IRM assay is useful in predicting virological response during PEG-IFN/RBV therapy.

Introduction

Recently, global consensus has been reached that a combination of interferon (IFN) or pegylated IFN plus ribavirin (PEG-IFN/RBV) is the treatment of choice for chronic hepatitis C. Even with this treatment regimen, however, sustained virological response (SVR) for those infected with the most resistant genotypes, hepatitis C virus (HCV)-1a and -1b, still hover at ~50% [1, 2]. Thus,

KARGER

Fax +41 61 306 12 34
E-Mail karger@karger.ch
www.karger.com

0300–5526/08/0517–0070$24.50/0

Accessible online at:
www.karger.com/int

Soo Ryang Kim, MD
Department of Gastroenterology, Kobe Asahi Hospital
3-5-25 Bououji-cho, Nagata-ku
Kobe 653-0801 (Japan)
Tel. +81 78 612 5151, Fax +81 78 612 5152, E-Mail asahi-hp@arion.ocn.ne.jp

it is worthy to identify the predictive factors that allow the selection of patients who would achieve the eradication of HCV RNA either before or during therapy, especially since IFN/RBV combination therapy is costly and has several side effects [3].

Predictors of IFN-based therapy can be classified into pre- and on-treatment factors. Pre-treatment factors comprise (1) host factors, such as age, gender, obesity, alcohol consumption, hepatic iron overload, fibrosis, immune responses and co-infection with other viruses, and (2) viral factors that mainly include viral genotypes, particular amino acid sequence variations in the NS5A region [4, 5] and in the core protein region of HCV [6] within a given genotype and the viral load. On-treatment factors are mainly related to viral kinetics within the first few weeks of treatment [7].

Although the detection of HCV RNA by reverse transcription-polymerase chain reaction (RT-PCR) represents the most sensitive method for determining persistent HCV infection, the assay is time-consuming, costly and technically demanding. In contrast, enzyme immunoassays (EIAs) for detecting HCV core antigen are simple and relatively inexpensive. A number of reports have demonstrated the utility of measuring HCV core antigen using EIAs [8–11]. Moreover, a new immunoradiometric (IRM) assay for detecting HCV core antigen has recently been developed [12].

In this study, we assessed the usefulness of the new IRM assay for HCV core antigen in efficiently predicting SVR, based on virological dynamics at 24 h, and 1, 2 and 4 weeks after the start of PEG-IFN/RBV combination therapy, in patients with HCV-1b ≥100 KIU/ml.

Patients and Methods

Between December 2004 and July 2006, 39 patients included in this study demonstrated high viral loads (>100 KIU/ml) of serum HCV RNA of genotype 1b; they had been diagnosed with chronic hepatitis C on the basis of abnormal serum alanine aminotransferase persisting for at least 6 months and positive HCV RNA assessed by RT-PCR. None of the patients was positive for hepatitis B surface antigen or other liver diseases (autoimmune hepatitis or alcoholic liver disease). All the patients received a regimen of PEG-IFNα-2b (Peg-Intron; Schering-Plough, Kenilworth, N.J., USA; 1.5 μg/kg/week, s.c.) in combination with RBV (Rebetol; Schering-Plough; 600–1,000 mg/day) for 48 weeks. RBV was administered at a dose of 600 mg/day (three capsules) to patients weighing <60 kg, 800 mg/day (four capsules) to those weighing <80 kg, and 1,000 mg/day (five capsules) to those weighing ≥80 kg.

The efficacy of the combination therapy was evaluated by HCV RNA negativity based on qualitative RT-PCR analysis at the end of therapy (end of therapy response) and 6 months after the completion of therapy (SVR). The amount of HCV RNA was measured quantitatively by RT-PCR (Amplicor HCV monitor; version 2.0; Roche, Basel, Switzerland) before therapy. The lower detection limit of the assay was 5 KIU/ml. Samples collected during and after therapy were also checked by qualitative RT-PCR (Amplicor, Roche), which has a higher sensitivity than quantitative analysis, and the results were labeled as positive or negative. The lower limit of the assay was 50 KIU/ml.

SVR was defined as undetectable serum HCV RNA 24 weeks after cessation of treatment, partial response (PR) as undetectable HCV RNA at the end of treatment, but positive 24 weeks after discontinuation of treatment, and no response (NR) as detectable HCV RNA at the end of treatment. Informed consent was obtained from all patients enrolled in the study after a thorough explanation of the aims, risks and benefits of the therapy.

The amount of HCV core antigen was assessed by the IRM assay (Ortho Clinical Diagnostics, Tokyo, Japan). The HCV core antigen assay has a detection limit of 20 fmol/l, as established by the manufacturer. HCV core antigen was measured on days 0, 1, 7 (1 week), 14 (2 weeks) and 28 (4 weeks).

Statistical Analysis

Differences between the groups were assessed by non-parametric tests (Mann-Whitney test, χ^2 test and Fisher's exact test). $p < 0.05$ was considered statistically significant.

Results

Of the 39 patients treated with combination therapy, 18 (46.2%) achieved SVR and 21 were still HCV RNA positive 6 months after therapy. Of the latter, 11 (28.2%) relapsed after the end of therapy (PR) and 10 (25.6%) showed NR. Patient characteristics (table 1) showed no significant differences among the three groups (NR, PR and SVR) except for the degree of fibrosis.

A good correlation was observed between the amount of HCV core antigen and the amount of HCV RNA in 39 samples at the start of therapy ($r^2 = 0.648$; fig. 1).

The time course of HCV RNA eradication during therapy showed no significant difference between PR and SVR (fig. 2). In the NR, PR and SVR groups, the amounts of HCV core antigen during the initial 4 weeks of therapy (fig. 3) were as follows: 12,781 ± 18,444, 7,875 ± 3,418 and 5,809 ± 5,919 fmol/l, at the start of therapy; 3,382 ± 4,903, 681 ± 721 and 426 ± 698 fmol/l, on day 1; 6,177 ± 6,682, 1,540 ± 2,376 and 393 ± 469 fmol/l, on day 7; 7,048 ± 10,323, 525 ± 953 and 135 ± 166 fmol/l, on day 14, and 3,543 ± 5,363, 168 ± 395 and 29 ± 19 fmol/l, on day 28, respectively. On days 1 and 7, there was a significant difference between SVR and PR ($p < 0.05$). At all points of time, the difference in the amount of HCV core antigen was significant between NR and SVR ($p < 0.05$), but not between PR and NR.

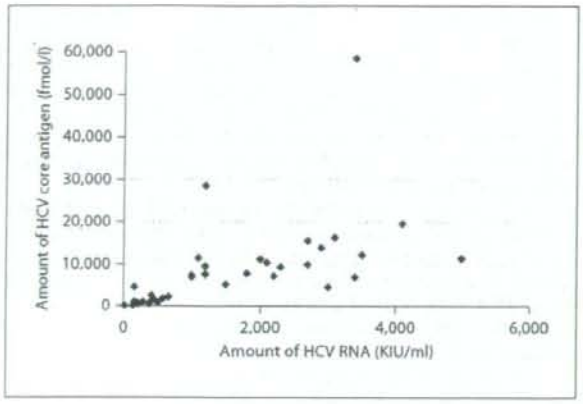

Fig. 1. Correlation between the amount of HCV core antigen and the amount of HCV RNA at the start of PEG-IFN/RBV combination therapy. There was a significant positive correlation (r^2 = 0.648, p = 0.0002. y = 4.48x + 1,470).

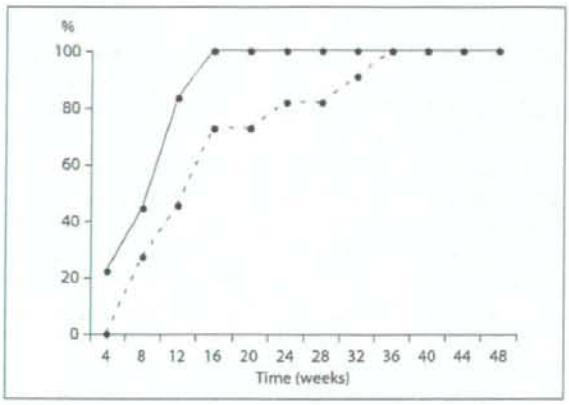

Fig. 2. Time course of HCV RNA eradication during PEG-IFN/RBV combination therapy. No significant difference was observed between SVR (——) and PR (– – –).

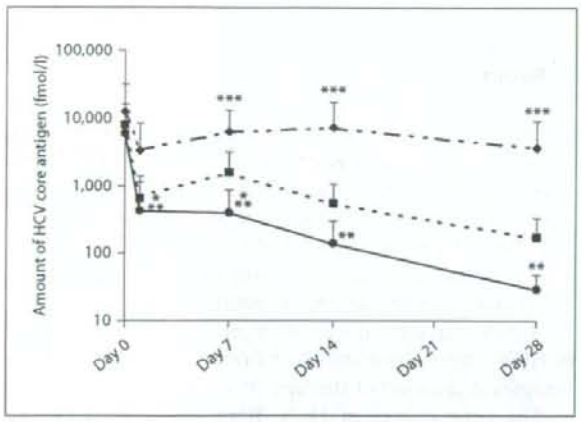

Fig. 3. Amount of HCV core antigen during PEG-IFN/RBV combination therapy. —— = SVR; – – – = PR; – – – – – = NR. * $p < 0.05$, SVR vs. PR; ** $p < 0.05$, SVR vs. NR, and *** $p < 0.05$, NR vs. PR.

Four weeks after the start of therapy, the following reductions in the amount of HCV core antigen were observed: a 1-log reduction in 20% (2/10) of the NR group, in 91% (10/11) of the PR group and in 88.9% (16/18) of the SVR group, and a 2-log reduction in 0% (0/10) of the NR group, in 63.6% (7/11) of the PR group and in 55.6% (10/18) of the SVR group (table 2).

Discussion

HCV core antigen, first detected in the circulation of HCV-infected hosts by EIA-based methods [13], had some limitations, in that levels under 20 fmol/l of HCV RNA could not be detected. Consequently, the methods were limited to the monitoring of late events during and after antiviral treatment. A modified version of the EIA developed for HCV core antigen [11] easily exposes the epitope of HCV core antigen, and the binding by anti-HCV core antibody in the serum can be reduced by incubation with three types of detergents. Since the modified EIA requires only one pretreatment step, it is simpler than the first-generation versions; moreover, it is 100-fold more sensitive. The second-generation EIA for HCV core antigen is useful in the diagnosis of acute and chronic hepatitis C and in predicting and monitoring the effect of IFN treatment [14].

Recently, a new IRM assay-based test for detecting HCV core antigen, a further modification of the EIA method of Aoyagi et al. [11], overcomes the effects of the serological HCV genotype group at the level of HCV core antigen detectable by EIA in serum. The sensitivity and specificity of the IRM assay are 96.4 and 100%, respectively. The sensitivity is similar between HCV serotype I (HCV genotypes 1a and 1b; 97.6%) and HCV serotype II (HCV genotypes 2a and 2b; 94.0%) [12].

Furthermore, the cost of the IRM assay kit is less than one third of the RT-PCR assay. Thus, this new IRM assay

Table 1. Host-dependent, virus-related profile

	NR	PR	SVR	p
Gender, males/females	6/4	7/4	9/9	NS
Age, years	59.8 ± 9.9	63.5 ± 7.3	55.5 ± 9.4	NS
HCV RNA level, KIU/ml	1,185 ± 1,154	2,093 ± 1,355	1,328 ± 1,321	NS
HCV core antigen, fmol/l	12,781 ± 18,444	7,875 ± 3,418	5,809 ± 5,919	NS
Body weight, kg	61.2 ± 11.2	60.8 ± 14.5	57.5 ± 9.6	NS
Treatment history (retreatment/naïve)	6/4	4/7	7/11	NS
Body mass index	23.7 ± 3.7	22.7 ± 3.7	22.4 ± 9.6	NS
F0–1/F2–3	3/6	1/6	14/3	0.003

is an economically valuable option for monitoring the amount of HCV in patients with chronic HCV infection. Indeed, in our study, there was a strong correlation between the amount of HCV core antigen in serum by the IRM assay and the amount of HCV RNA in serum measured by quantitation RT-PCR ($r^2 = 0.648$).

Although some studies have suggested that quantitative HCV RNA determinations allow earlier assessment of treatment response, the assays were not generally available commercially, and they were not standardized. Therefore, we used the IRM assay to predict virological response during PEG-IFN/RBV therapy in patients with HCV-1b ≥100 KIU/ml.

To be able to assess whether long-term response is attainable as early as possible during the treatment course, and to have the option of discontinuing treatment in cases where virological response is not expected, is desirable. This strategy has the potential of making a trial more appealing to patients by providing a limited 'test' period of treatment before committing to a full course of therapy [6].

The accuracy of the degree of viral inhibition, during the early weeks of treatment (early virological response: EVR) with PEG-IFNα-2b/RBV, has been examined to identify patients who would not respond to therapy. The best definition of EVR is a reduction in HCV RNA by at least 2 log after the first 12 weeks of treatment compared with baseline. Depending on the treatment regimen, between 69 and 76% of patients have achieved this threshold, with SVR attained in 67–80% [15].

The importance of EVR has been emphasized in predicting SVR and non-SVR: patients who do not reach EVR are not responsive to further therapy. Discontinuation of treatment in patients not reaching EVR would reduce drug costs by >20%; consequently, early confirmation of viral reduction after initiating antiviral therapy for chronic hepatitis C is worthwhile [16].

Table 2. Reduction in the amount of HCV RNA 4 weeks after the start of PEG-IFN/RBV therapy

Reduction	NR	PR	SVR
1 log	20% (2/10)	91% (10/11)	88.9% (16/18)
2 log	0% (0/10)	63.6% (7/11)	55.6% (10/18)

Treatment with IFN results in a decline in HCV RNA levels, which can be resolved mathematically into two phases. The first-phase decline is usually measured at 24 or 48 h, and probably reflects direct inhibition of intracellular HCV production and release [17], with IFN efficacy ranging from about 70% (approximately 0.7 log units) for standard IFN given three times a week to more than 90% (1 log units) for high daily doses of standard IFN or PEG-IFN once a week [18, 19]. The second-phase decline begins after 24–48 h, is slower and more variable than the first phase, and is thought to reflect continued inhibition of replication and the gradual elimination of virus-infected cells [17]. The decay correlates less with the IFN dose than the first phase, but is more rapid with PEG-IFN as compared with standard IFN preparations [16].

Lowering HCV RNA during the first phase is essential for efficient elimination of HCV during the second phase. Decreases in HCV RNA titers within the first 24–48 h after the start of IFN, therefore, would be dependable estimates of antiviral efficacy [18, 19].

As observed with the first phase, RBV does not appear to influence second-phase kinetics [16]. Four weeks after

the start of therapy, a 1-log reduction was observed in 20% (2/10) of NR patients, 91% (10/11) of PR and 88.9% (16/18) of SVR, and a 2-log reduction in 0% (0/10) of NR, 63.6% (7/11) of PR and 55.6% (10/18) of SVR patients. These results indicate that the reduction of 1 and 2 log in the amount of HCV core antigen 4 weeks after therapy is not a defining condition for PR and SVR. There are two kinds of non-SVR (PR and NR): PR is defined as HCV RNA undetectable at the end of treatment and positive 24 weeks after the discontinuation of therapy; NR is defined as HCV RNA detectable at the end of treatment.

At all points of time, a significant difference was observed in the amount of HCV core antigen between SVR and NR. Accordingly, SVR can easily be differentiated from NR by IRM assay during therapy. With regard to the time course of HCV RNA eradication, however, there is no difference between PR and SVR. The prediction of SVR and PR by the earliest possible use of the IRM assay is desirable.

In our study, 1 and 7 days after the start of therapy, there was a significant difference in the amount of HCV core antigen between SVR and PR. Our finding that SVR and PR could be differentiated by the IRM assay during the first and second phases is very useful for clinicians engaged in the treatment of C-type hepatitis, because PR patients should be treated for 72 weeks in order to maximize the probability of SVR [20, 21].

Taken together, our results demonstrate that early viral dynamics, such as changes in the amount of HCV core antigen detected by the IRM assay in the first and second phases during PEG-IFNα-2b/RBV therapy, predict outcome not only between SVR and NR but also between SVR and PR. Since the number of patients was small in our study, further studies including larger patient cohorts are needed to confirm the promising potential of the IRM assay.

In conclusion, this new IRM assay is useful in predicting virological response during PEG-IFN/RBV combination therapy administered for chronic hepatitis C with high viral loads of HCV RNA genotype 1b.

Acknowledgments

This study was also carried out as part of the Program of Founding Research Centers for Emerging and Reemerging Infectious Diseases. We are indebted to K. Ohyama and Y. Kawamura for their assistance in the preparation of the manuscript.

Disclosure Statements

The authors have no disclosures to make.

References

1 Fried MW, Shiffman ML, Reddy KR, Smith C, Marinos G, Goncales FL Jr, Haussinger D, Diago M, Carosi G, Dhumeaux D, Craxi A, Lin A, Hoffman J, Yu J: Peginterferon alfa-2a plus ribavirin for chronic hepatitis C virus infection. N Engl J Med 2002;26:975–982.

2 Manns MP, McHutchison JG, Gordon SC, Rustgi VK, Shiffman M, Reindollar R, Goodman ZD, Koury K, Ling M, Albrecht JK: Peginterferon alfa-2b plus ribavirin compared with interferon alfa-2b plus ribavirin for initial treatment of chronic hepatitis C: randomized trial. Lancet 2001;22:958–965.

3 Nakamura H: Early prediction of sustained viral responder and non-responder during interferon and ribavirin combination therapy in chronic hepatitis C. Hepatol Res 2005; 33:269–271.

4 El-Shamy A, Sasayama M, Nagano-Fujii M, Sasase N, Imoto S, Kim SR, Hotta H: Prediction of efficient virological response to pegylated interferon/ribavirin combination therapy by NS5A sequences of hepatitis C virus and anti-NS5A antibodies in pre-treatment sera. Microbiol Immunol 2007;51:471–482.

5 Enomoto N, Sakuma I, Asahina Y, Kurosaki M, Murakami T, Yamamoto C, Ogura Y, Izumi N, Marumo F, Sato C: Mutations in the nonstructural protein 5A gene and response to interferon in patients with chronic hepatitis C virus 1b infection. N Engl J Med 1996; 334:77–81.

6 Akuta N, Suzuki S, Kawamura Y, Yatsuji H, Sezaki H, Suzuki Y, Hosaka T, Kobayashi M, Kobayashi M, Arase Y, Ikeda K, Miyakawa Y, Kumada H: Prediction of response to pegylated interferon and ribavirin in hepatitis C by polymorphism in the viral core protein and very early dynamics of viremia. Intervirology 2007;50:361–368.

7 Ferenci P: Predictors of response to therapy for chronic hepatitis C. Semin Liver Dis 2004;24:S25–S31.

8 Dickson RC, Mizokami M, Orito E, Qian KP, Lau JY: Quantification of serum HCV core antigen by a fluorescent enzyme immunoassay in liver transplant recipients with recurrent hepatitis C – clinical and virologic implications. Transplantation 1999;68:1512–1516.

9 Komatsu F, Takahashi K: Determination of serum hepatitis C (HCV) core protein using a novel approach for quantitative evaluation of HCV viremia in anti-HCV-positive patients. Liver 1999;19:375–380.

10 Widell A, Molnegren V, Pieksma F, Calmann M, Peterson J, Lee SR: Detection of hepatitis C core antigen in serum or plasma as a marker of hepatitis C viremia in the serological window-phase. Transfus Med 2002;12:107–113.

11 Aoyagi K, Ohue C, Iida K, Kimura T, Tanaka E, Kiyosawa K, Yagi S: Development of a simple and highly sensitive enzyme immunoassay for hepatitis C virus core antigen. J Clin Microbiol 1999;37:1802–1808.

12 Hayashi K, Hasuike S, Kusumoto K, Ido A, Uto H, Kenji N, Kohara M, Stuver SO: Usefulness of a new immuno-radiometric assay to detect hepatitis C core antigen in a community-based population. J Viral Hepat 2005;12:106–110.

13 Tanaka T, Lau JYN, Mizokami M, Orito E, Tanaka E, Kiyosawa K, Yasui K, Ohta Y, Hasegawa A, Tanaka S, et al: Simple fluorescent enzyme immunoassay for detection and quantification of hepatitis C viremia. J Hepatol 1995;23:742–745.
14 Tanaka E, Ohue C, Aoyagi K, Yamaguchi K, Yagi S, Kiyosawa K, Alter HJ: Evaluation of a new enzyme immunoassay for hepatitis C virus (HCV) core antigen with clinical sensitivity approximating that of genomic amplification of HCV RNA. Hepatology 2000;32:388–393.
15 Davis GL, Wong JB, McHutchison JG, Manns MP, Harvey J, Albrecht J: Early virologic response to treatment with peginterferon alfa 2b plus ribavirin in patients with chronic hepatitis C. Hepatology 2003;38:645–652.
16 Davis GL: Monitoring of viral levels during therapy of hepatitis C. Hepatology 2002;36:S145–S151.
17 Neumann AU, Lam NP, Dahari H, Gretch DR, Wiley TE, Layden TJ, Perelson AS: Hepatitis C viral dynamics in vivo and the antiviral efficacy of interferon-α therapy. Science 1998;282:103–107.
18 Lam NP, Neumann AU, Gretch DR, Wiley TE, Perelson AS, Layden TJ: Dose-dependent acute clearance of hepatitis C genotype 1 virus with interferon alfa. Hepatology 1997;26:226–231.
19 Zeuzem S, Herrmann E, Lee JH, Fricke J, Neumann AU, Modi M, Colucci G, Roth WK: Viral kinetics in patients with chronic hepatitis C treated with standard or peginterferon alfa-2a. Gastroenterology 2001;120:1438–1447.
20 Buti M, Valdes A, Sanchez-Avila F, Esteban R, Lurie Y: Extending combination therapy with peginterferon alfa-2b plus ribavirin for genotype 1 chronic hepatitis C late responders: a report of 9 cases. Hepatology 2003;37:1226–1227.
21 Berg T, von Wagner M, Nasser S, Sarrazin C, Heintges T, Gerlach T, Buggisch P, Goeser T, Rasenack J, Pape GR, Schmidt WE, Kallinowski B, Klinker H, Spingler U, Martus P, Alshuth U, Zeuzem S: Extended treatment duration for hepatitis C virus type 1: comparing 48 versus 72 weeks of peginterferon-alfa-2a plus ribavirin. Gastroenterology 2006;130:1086–1097.

JOURNAL OF VIROLOGY, Nov. 2008, p. 10375–10385 Vol. 82, No. 21
0022-538X/08/$08.00+0 doi:10.1128/JVI.00395-08

Hepatitis C Virus Infection Induces Apoptosis through a Bax-Triggered, Mitochondrion-Mediated, Caspase 3-Dependent Pathway▽

Lin Deng,[1] Tetsuya Adachi,[1] Kikumi Kitayama,[1] Yasuaki Bungyoku,[1] Sohei Kitazawa,[2] Satoshi Ishido,[3] Ikuo Shoji,[1] and Hak Hotta[1]*

Divisions of Microbiology[1] and Molecular Pathology,[2] Kobe University Graduate School of Medicine, 7-5-1 Kusunoki-cho, Chuo-ku, Kobe 650-0017, and Laboratory for Infectious Immunity, Riken Research Center for Allergy and Immunology, 1-7-22 Suehiro-cho, Tsurumi-ku, Yokohama, Kanagawa 230-0045,[3] Japan

Received 23 February 2008/Accepted 20 August 2008

We previously reported that cells harboring the hepatitis C virus (HCV) RNA replicon as well as those expressing HCV NS3/4A exhibited increased sensitivity to suboptimal doses of apoptotic stimuli to undergo mitochondrion-mediated apoptosis (Y. Nomura-Takigawa, et al., J. Gen. Virol. 87:1935–1945, 2006). Little is known, however, about whether or not HCV infection induces apoptosis of the virus-infected cells. In this study, by using the chimeric J6/JFH1 strain of HCV genotype 2a, we demonstrated that HCV infection induced cell death in Huh7.5 cells. The cell death was associated with activation of caspase 3, nuclear translocation of activated caspase 3, and cleavage of DNA repair enzyme poly(ADP-ribose) polymerase, which is known to be an important substrate for activated caspase 3. These results suggest that HCV-induced cell death is, in fact, apoptosis. Moreover, HCV infection activated Bax, a proapoptotic member of the Bcl-2 family, as revealed by its conformational change and its increased accumulation on mitochondrial membranes. Concomitantly, HCV infection induced disruption of mitochondrial transmembrane potential, followed by mitochondrial swelling and release of cytochrome *c* from mitochondria. HCV infection also caused oxidative stress via increased production of mitochondrial superoxide. On the other hand, HCV infection did not mediate increased expression of glucose-regulated protein 78 (GRP78) or GRP94, which are known as endoplasmic reticulum (ER) stress-induced proteins; this result suggests that ER stress is not primarily involved in HCV-induced apoptosis in our experimental system. Taken together, our present results suggest that HCV infection induces apoptosis of the host cell through a Bax-triggered, mitochondrion-mediated, caspase 3-dependent pathway(s).

Hepatitis C virus (HCV) often establishes persistent infection to cause chronic hepatitis, liver cirrhosis, and hepatocellular carcinoma, which is a significant health problem around the world (56). Although the exact mechanisms of HCV pathogenesis, such as viral persistence, liver cell injury, and carcinogenesis, are not fully understood yet, an accumulating body of evidence suggests that apoptosis of hepatocytes is significantly involved in the pathogenesis of HCV (1, 2, 9). It is widely accepted that apoptosis of virus-infected cells is an important strategy of the host to protect itself against viral infections. Apoptotic cell death can be mediated either by the host immune responses through the function of virus-specific cytotoxic T lymphocytes and/or by viral proteins themselves that trigger an apoptotic pathway(s) of the host cell.

Apoptotic pathways can be classified into two groups: the mitochondrial death (intrinsic) pathway and the extrinsic cell death pathway initiated by the tumor necrosis factor (TNF) family members (31, 63). Mitochondrion-mediated apoptosis is initiated by a variety of apoptosis-inducing signals that cause the imbalance of the major apoptosis regulator, the proteins of the Bcl-2 family, such as Bcl-2, Bax, and Bid. For example, the proapoptotic protein Bax accumulates on mitochondria after being activated and triggers an increase in the permeability of the outer mitochondrial membrane. Consequently, the mitochondria release cytochrome *c* and other key molecules that facilitate apoptosome formation to activate caspase 9. This, in turn, activates downstream death programs, such as caspase 3 and poly(ADP-ribose) polymerase (PARP). The mitochondria also release apoptosis-inducing factor and endonuclease G to facilitate caspase-independent apoptosis. On the other hand, the extrinsic cell death pathway involves the activation of caspase 8 through binding to the adaptor protein Fas-associated protein with death domain (FADD), which in turn activates caspase 3 to facilitate cell death.

There have been many studies regarding the HCV protein(s) that is directly involved in apoptosis, identifying the protein as either proapoptotic or antiapoptotic, and some data are inconsistent. For example, core (5, 13, 36, 73), E1 (15, 16), E2 (12), NS3 (48), NS4A (43), and NS5A and NS5B (57) have been reported to induce apoptosis. On the other hand, there are reports showing that core (40, 49, 51), E2 (35), NS2 (21), NS3 (58), and NS5A (33, 67) function as antiapoptotic proteins. However, whether the virus as a whole is proapoptotic or antiapoptotic needs to be studied in the context of virus replication, which is believed to be much more dynamic than mere expression of a viral protein(s).

We previously reported that replication of an HCV RNA replicon rendered the host cell prone to undergoing mitochondrion-mediated apoptosis upon suboptimal doses of apoptosis-inducing stimuli (43). Recently, an efficient virus infection system using a particular clone of HCV genotype 2a and a highly permissive human hepatocellular carcinoma-derived cell line

* Corresponding author. Mailing address: Division of Microbiology, Kobe University Graduate School of Medicine, 7-5-1 Kusunoki-cho, Chuo-ku, Kobe 650-0017, Japan. Phone: 81-78-382-5500. Fax: 81-78-382-5519. E-mail: hotta@kobe-u.ac.jp.

▽ Published ahead of print on 3 September 2008.

has been developed (37, 38, 66, 71). In this study, by using the virus infection system, we examined the possible effect of HCV infection on the fate of the host cell. We report here that HCV infection induces apoptosis via the mitochondrion-mediated pathway, as demonstrated by the increased accumulation of the proapoptotic protein Bax on the mitochondria, decreased mitochondrial transmembrane potential, and mitochondrial swelling, which result in the release of cytochrome *c* from the mitochondria and the activation of caspase 3.

MATERIALS AND METHODS

Cells. The Huh7.5 cell line (6), a highly HCV-susceptible subclone of Huh7 cells, was a kind gift from C. M. Rice, Center for the Study of Hepatitis C, The Rockefeller University. The cells were propagated in Dulbecco's modified Eagle medium supplemented with 10% heat-inactivated fetal bovine serum and 0.1 mM nonessential amino acids.

Virus. The virus stock used in this study was prepared as described below. The pFL-J6/JFH1 plasmid, encoding the entire viral genome of a chimeric strain of HCV genotype 2a, J6/JFH1 (37), was kindly provided by C. M. Rice. The plasmid was linearized by XbaI digestion and in vitro transcribed by using T7 RiboMAX (Promega, Madison, WI) to generate the full-length viral genomic RNA. The in vitro-transcribed RNA (10 μg) was transfected into Huh7.5 cells by means of electroporation (975 μF, 270 V) using Gene Pulser (Bio-Rad, Hercules, CA). The cells were then cultured in complete medium, and the supernatant was propagated as an original virus (J6/JFH1-passage 1 [J6/JFH1-P1]). Since the infectious titer of the original virus was not high enough for infection of all the cells in the culture at once, an adapted strain of the virus was obtained by passaging the virus-infected cells 47 times. The adapted virus (J6/JFH1-P47), which is a pool of adapted mutants, possesses 10 amino acid mutations (K78E, T396A, T416A, N534H, A712V, Y852H, W879R, F2281L, M2876L, and T2925A) and a single nucleotide mutation in the 5′-untranslated region (U146A) and produces a much higher titer of infectivity in Huh7.5 cell cultures than the original J6/JFH1-P1 (our unpublished data). Virus infection was performed at a multiplicity of infection of 2.0. Culture supernatants of uninfected cells served as a control (mock preparation).

Virus infectivity was measured by indirect immunofluorescence analysis, as described below, and expressed as cell-infecting units/ml.

Cell viability/proliferation assay. Huh7.5 cells were seeded in 96-well plates at a density of 1.0×10^4 cells/well and cultured overnight. The cells were then infected with the virus or the mock preparation, and, at different time points, cell viability/proliferation was determined by the WST-1 assay (Roche, Mannheim, Germany), as described previously (43).

Detection of apoptosis. The degree of apoptosis was measured by using a Cell Death Detection ELISA^{Plus} kit (Roche), which is based on the determination of cytoplasmic histone-associated DNA fragments, according to the manufacturer's protocol. In brief, cells cultured in a 96-well plate were centrifuged at $200 \times g$ for 10 min at 4°C to remove the supernatant. After the cells were lysed with lysis buffer, the plate was centrifuged at $200 \times g$ for 10 min to separate the cytoplasmic and nuclear fractions. Twenty microliters of supernatant was placed in each well of a streptavidin-coated 96-well plate. Subsequently, a mixture of biotin-labeled anti-histone antibody and peroxidase-labeled anti-DNA antibody was added and wells were incubated for 2 h at room temperature. After wells were washed three times to remove the unbound components, peroxidase activities were determined photometrically with 2,2′-azino-diethyl-benzthiazolin sulfonate as a substrate and measured by using a microplate reader (Bio-Rad).

Caspase enzymatic activities. Activities of caspase 3, 8, and 9 were measured by using Caspase-Glo 3/7, 8, and 9 assays (Promega), respectively, according to the manufacturer's instructions. In brief, a proluminescence caspase 3/7, 8, or 9 substrate, which consists of aminoluciferin (substrate for luciferase) and the tetrapeptide sequence DEVD, LETD, or LEHD (cleavage site for caspase 3/7, 8, or 9, respectively), was added to cultured cells in each well of a 96-well plate, and the plate was incubated for 30 min at room temperature. In the presence of caspase 3/7, 8, or 9, aminoluciferin was liberated from the proluminescence substance and utilized as a substrate for the luciferase reaction. The resultant luminescence in relative light units was measured by using a Luminescencer-JNR AB-2100 (Atto, Tokyo, Japan).

Cell fractionation. Cells were fractionated by using a mitochondrial isolation kit (Pierce, Rockford, IL), according to the manufacturer's instructions. Briefly, 2×10^7 cells were harvested and suspended in reagent A containing a protease inhibitor cocktail (Roche). The cell suspension was mixed with buffer B, vortexed for 5 min, and then mixed with reagent C. The nuclei and unbroken cells were removed by centrifugation at $700 \times g$ for 10 min at 4°C, and the supernatant was used as cell lysate. The cell lysate was further centrifuged at $3,000 \times g$ for 15 min at 4°C. The pellet obtained, which was considered the mitochondrial fraction, was washed once with reagent C and dissolved in a lysis buffer containing 10 mM Tris-HCl (pH 7.5), 150 mM NaCl, 1 mM EDTA, 1% NP-40, and a protease inhibitor cocktail. The remaining supernatant was further centrifuged at $100,000 \times g$ for 30 min at 4°C, and the resultant supernatant was collected as a cytosolic fraction.

To verify successful mitochondrial fractionation, the cytosolic and mitochondrial fractions were analyzed by immunoblotting, as described below, using antibody against Tim23, a mitochondrion-specific protein.

Analysis of the mitochondrial transmembrane potential. The mitochondrial transmembrane potential was measured by flow cytometry using the cationic lipophilic green fluorochrome rhodamine 123 (Rho123; Sigma, St. Louis, MO), as described previously (43). Briefly, cells (7×10^5) were harvested, washed twice with phosphate-buffered saline (PBS), and incubated with Rho123 (0.5 μg/ml) at 37°C for 25 min. The cells were then washed twice with PBS, and Rho123 intensity was analyzed by a flow cytometer (Becton Dickinson, San Jose, CA). A total of 10,000 events were collected per sample. Mean fluorescence intensities were measured by calculating the geometric mean for each histogram peak.

Detection of morphological changes of the mitochondria. Mitochondrial morphology was analyzed by two different methods. (i) For fluorescence microscopy, Huh7.5 cells seeded on glass coverslips in a 24-well plate were incubated for 30 min at 37°C with 100 nM MitoTracker (Molecular Probes, Eugene, OR). After being washed twice with PBS, the cells were fixed with 3.7% paraformaldehyde and observed under a confocal laser scanning microscope (Carl Zeiss, Oberkochen, Germany). When needed, the fixed cells were subjected to indirect immunofluorescence to confirm HCV infection, as described below. (ii) Electron microscopy was performed as described previously (23, 43). In brief, cells were fixed with 4% paraformaldehyde and 0.2% glutaraldehyde for 30 min at room temperature. After being washed with PBS, the cells were collected, dehydrated in a series of 70%, 80%, and 90% ethanol, embedded in LR White resin (London Resin, Berkshire, United Kingdom), and kept at −20°C for 2 days to facilitate resin polymerization. After ultrathin sectioning, samples were etched in 3% H_2O_2 for 5 min at room temperature and washed with PBS. Sections were stained with uranyl acetate and lead citrate and observed under a transmission electron microscope (JEM 1299EX; JOEL, Tokyo, Japan).

Detection of mitochondrial superoxide. Cells seeded on glass coverslips in a 24-well plate were incubated with 5 μM MitoSOX Red (Molecular Probes) at 37°C for 10 min. After being washed with warm Hanks' balanced salt solution with calcium and magnesium (Invitrogen, Carlsbad, CA), the cells were fixed with 3.7% paraformaldehyde and observed under a confocal laser scanning microscope (Carl Zeiss). When needed, the fixed cells were subjected to indirect immunofluorescence to confirm HCV infection, as described below.

Indirect immunofluorescence. Cells seeded on glass coverslips in a 24-well plate at a density of 6×10^4 cells/well were infected with HCV or left uninfected. At different time points after virus infection, the cells were fixed with 3.7% paraformaldehyde in PBS for 15 min at room temperature and permeabilized in 0.1% Triton X-100 in PBS for 15 min at room temperature. After being washed with PBS twice, cells were consecutively stained with primary and secondary antibodies. Primary antibodies used were anti-active caspase 3 rabbit polyclonal antibody (Promega) and an HCV-infected patient's serum. Secondary antibodies used were Cy3-conjugated donkey anti-rabbit immunoglobulin G (IgG; Chemicon, Temecula, CA), Alexa Fluor 594-conjugated goat anti-human IgG (Molecular Probes), and fluorescein isothiocyanate (FITC)-conjugated goat anti-human IgG (MBL, Nagoya, Japan). The cells were washed with PBS, counterstained with Hoechst 33342 solution (Molecular Probes) at room temperature for 10 min, mounted on glass slides, and observed under a confocal laser scanning microscope (Carl Zeiss). The specificity of this immunostaining was confirmed by using mouse monoclonal antibody against HCV core protein (C7-50; Abcam, Tokyo, Japan).

To analyze the possible localization of the activated Bax on mitochondrial membranes, cells were incubated with MitoTracker and subjected to immunofluorescence analysis using rabbit polyclonal antibody against activated Bax (NT antibody; Upstate, Lake Placid, NY). This antibody is directed toward N-terminal residues 1 to 21 of Bax in an N-terminal conformation-dependent manner and specifically recognizes the active form of Bax, in which this segment is exposed in response to apoptotic stimuli (64).

Immunoblotting. Cells were lysed in a buffer containing 10 mM Tris-HCl (pH 7.5), 150 mM NaCl, 1 mM EDTA, 1% NP-40, and a protease inhibitor cocktail (Roche). After two freeze-thaw cycles, cell debris was removed by

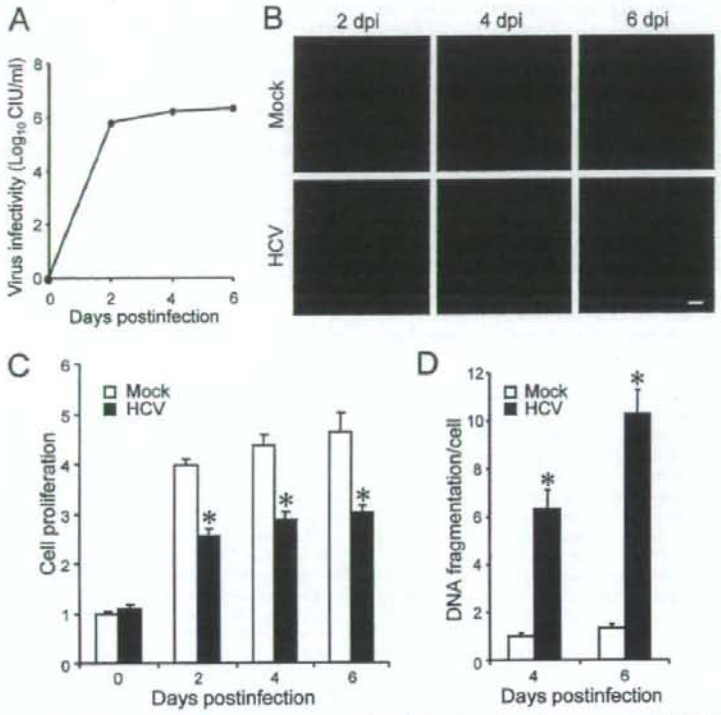

FIG. 1. HCV infection induces apoptosis in Huh7.5 cells. (A) Virus infectivity in the culture supernatants of HCV-infected cells. (B) Detection of HCV antigens in the cells. Huh7.5 cells mock inoculated or inoculated with HCV were subjected to indirect immunofluorescence analysis to detect HCV antigens (red staining) using an HCV-infected patient's serum and Alexa Fluor 594-conjugated goat anti-human IgG at 2, 4, and 6 days postinfection (dpi). Nuclei were counterstained with Hoechst 33342 (blue staining). Scale bar, 50 μm. (C) Cell viability/proliferation was measured for HCV-infected cultures and the mock-inoculated controls. Proliferation of the control cells at day 0 postinfection was arbitrarily expressed as 1.0. Data represent means ± standard deviations (SD) of three independent experiments. *, $P < 0.01$, compared with the control. (D) DNA fragmentation was measured as an index of apoptotic cell death for HCV-infected cultures and the mock-inoculated controls. DNA fragmentation of the control cells at 4 days postinfection was arbitrarily expressed as 1.0. Data represent means ± SD of three independent experiments. *, $P < 0.01$, compared with the control.

centrifugation. Protein quantification was carried out using a bicinchoninic acid protein assay kit (Pierce). Equal amounts of soluble proteins (4 to 20 μg) were subjected to sodium dodecyl sulfate-polyacrylamide gel electrophoresis and transferred onto a polyvinylidene difluoride membrane (Millipore, Bedford, MA), which was then incubated with the respective primary antibody. The primary antibodies used were mouse monoclonal antibodies against cytochrome *c* (A-8; Santa Cruz Biotechnology, Santa Cruz, CA), HCV NS3 (Chemicon), Tim23, Bax and Bcl-2 (BD Biosciences Pharmingen, San Diego, CA); rabbit polyclonal antibodies against Bak (Upstate), caspase 3, and PARP (Cell Signaling Technology, Danvers, MA); and goat polyclonal antibodies against glucose-regulated protein 78 (GRP78) and GRP94 (Santa Cruz Biotechnology). Horseradish peroxidase-conjugated goat anti-mouse IgG (MBL), goat anti-rabbit IgG (Bio-Rad), and donkey anti-goat IgG (Santa Cruz Biotechnology) were used as secondary antibodies. In some experiments, a commercial kit that facilitates the antigen-antibody reaction (Can Get Signal; Toyobo, Osaka, Japan) was used to obtain stronger signals. The respective protein bands were visualized by means of an enhanced chemiluminescence (GE Healthcare, Buckinghamshire, United Kingdom), and the intensity of each band was quantified by using NIH Image J. Protein loading was normalized by probing with goat antibody against actin (Santa Cruz Biotechnology) as a primary antibody.

Statistical analysis. The two-tailed Student *t* test was applied to evaluate the statistical significance of differences measured from the data sets. A *P* value of <0.05 was considered statistically significant.

RESULTS

HCV infection induces caspase 3-dependent apoptosis in Huh7.5 cells. We first examined virus growth in Huh7.5 cells. HCV grew efficiently in the culture, and virus titers in the supernatant reached a plateau level at 2 days postinfection (Fig. 1A). Immunofluorescence analysis revealed that >95% of the cells were infected with HCV on the same day (Fig. 1B). To examine the possible impact of HCV infection on the cells, we measured the cell viability/proliferation at 0, 2, 4, and 6 days postinfection. As shown in Fig. 1C, the proliferation of HCV-infected cells was significantly slower than that of the mock-infected control. Similar results were obtained when the parental Huh7 cells were used for HCV infection (data not shown). The observed delay in cell proliferation was associated with an increase in cell death, seen as cell rounding and floating in the culture (data not shown) and in cellular DNA fragmentation (Fig. 1D). As DNA fragmentation is a hallmark of apoptosis, our data suggest that HCV infection induces apoptosis in Huh7.5 cells.

The J6/JFH1-P47 strain of HCV used in this study possesses adaptive mutations compared to the original strain (J6/JFH1-P1). Therefore, we compared the impacts of the two strains on cell viability/proliferation and DNA fragmentation. While both strains caused inhibition of cell proliferation and an increase in DNA fragmentation, J6/JFH1-P47 appeared to exert a stronger cytopathic effect than J6/JFH-P1 (data not shown).

To further verify that HCV infection induces apoptotic cell death, we analyzed caspase 3 activities in HCV-infected Huh7.5 cells and the mock-infected control. As shown in Fig. 2A, caspase 3 activities in HCV-infected cells increased to levels that were 2.2, 6.0, and 12 times higher than that in the control cells at 2, 4, and 6 days postinfection, respectively. We also examined HCV-induced caspase 3 activation by immunoblot analysis. Activation of caspase 3 requires proteolytic processing of its inactive proenzyme into the active 17-kDa and 12-kDa subunit proteins. The anti-caspase 3 antibody used in this analysis recognizes 35-kDa procaspase 3 and the 17-kDa subunit protein. At 6 days postinfection, activated caspase 3 was detected in HCV-infected cells but not in the mock-infected control (Fig. 2B, second row from the top). Analysis of the death substrate PARP, which is a key substrate for active caspase 3 (61), also demonstrated that the uncleaved PARP (116 kDa) was proteolytically cleaved to generate the 89-kDa fragment in HCV-infected cells but not in the mock-infected control (Fig. 2B, third row). Cleavage of PARP facilitates cellular disassembly and serves as a marker of cells undergoing apoptosis (44).

In order to further confirm these observations, indirect immunofluorescence staining was performed by using an anti-active caspase 3 antibody that specifically recognizes the newly exposed C terminus of the 17-kDa fragment of caspase 3 but not the inactive precursor form. As shown in Fig. 2C, the activated form of caspase 3 was clearly observed in HCV-infected cells but not in the mock-infected control at 6 days postinfection. The activation of caspase 3 was observed also at 4 days postinfection (data not shown). We found that caspase 3 activation was detectable in 12% and 21% of HCV antigen-positive cells at 4 and 6 days postinfection, respectively, whereas it was detectable only minimally in mock-infected cells at the same time points (Fig. 2D). These results strongly suggest that HCV-induced cell death is caused by caspase 3-dependent apoptosis. We also observed nuclear translocation of active caspase 3 in HCV-infected cells (Fig. 2E). This result is consistent with previous reports (28, 70) that activated caspase 3 is located not only in the cytoplasm but also in the nuclei of apoptotic cells. Concomitantly, nuclear condensation and shrinkage were clearly observed in the caspase 3-activated cells. As the activation and nuclear translocation of caspase 3 occur before the appearance of the nuclear change, not all caspase 3-activated cells exhibited the typical nuclear changes. Taken together, these results indicate that HCV-induced apoptosis is associated with activation and nuclear translocation of caspase 3.

HCV infection induces the activation of the proapoptotic protein Bax. The proteins of the Bcl-2 family are known to directly regulate mitochondrial membrane permeability and induction of apoptosis (63). Therefore, we examined the expression levels of proapoptotic proteins, such as Bax and Bak, and antiapoptotic protein Bcl-2 in HCV-infected Huh7.5 cells and the mock-infected control. The result showed that expression levels of Bak or Bcl-2 did not differ significantly between HCV-infected cells and the control. Interestingly, however, Bax accumulated on the mitochondria in HCV-infected cells to a larger extent than in the mock-infected control (Fig. 3A), with the average amount of mitochondrion-associated Bax in HCV-infected cells being 2.7 times larger than that in the control cells at 6 days postinfection (Fig. 3B).

In response to apoptotic stimuli, Bax undergoes a conformational change to expose its N and C termini, which facilitates translocation of the protein to the mitochondrial outer membrane (32). Thus, the conformational change of Bax represents a key step for its activation and subsequent apoptosis. We therefore investigated the possible conformational change of Bax in HCV-infected cells by using a conformation-specific NT antibody that specifically recognizes the Bax protein with an exposed N terminus. As shown in Fig. 3C, Bax staining with the conformation-specific NT antibody was readily detectable in HCV-infected cells at 6 days postinfection whereas there was no detectable staining with the same antibody in the mock-infected control. Moreover, the activated Bax was shown to be colocalized with MitoTracker, a marker for mitochondria, in HCV-infected cells. The conformational change of Bax was observed in 10% and 15% of HCV-infected cells at 4 and 6 days postinfection, respectively (Fig. 3D). This result was consistent with what was observed for caspase 3 activation in HCV-infected cells (Fig. 2D). Taken together, these results suggest that HCV infection triggers conformational change and mitochondrial accumulation of Bax, which lead to the activation of the mitochondrial apoptotic pathway.

HCV infection induces the disruption of the mitochondrial transmembrane potential, release of cytochrome *c* from mitochondria, and activation of caspase 9. The accumulation of Bax on the mitochondria is known to decrease the mitochondrial transmembrane potential and increase its permeability, which result in the release of cytochrome *c* and other key molecules from the mitochondria to the cytoplasm to activate caspase 9. Therefore, we examined the possible effect of HCV infection on mitochondrial transmembrane potential in Huh7.5 cells. Disruption of the mitochondrial transmembrane potential was indicated by decreased Rho123 retention and, hence, decreased fluorescence. As shown in Fig. 4, HCV-infected cells showed ~50% and ~70% reductions in Rho123 fluorescence intensity compared with the mock-infected control at 4 and 6 days postinfection, respectively.

Recent studies have indicated that loss of mitochondrial membrane potential leads to mitochondrial swelling, which is often associated with cell injury (27, 50). Also, we and other investigators have reported that HCV NS4A (43), core (53), and p7 (22) target mitochondria. We therefore analyzed the effect of HCV infection on mitochondrial morphology. Confocal fluorescence microscopic analysis using MitoTracker revealed that mitochondria began to undergo morphological changes at 4 days postinfection and that approximately 40% of HCV-infected cells exhibited mitochondrial swelling and/or aggregation compared with the mock-infected control at 6 days postinfection (Fig. 5A and B). It should also be noted that mitochondrial swelling and/or aggregation was seen in a region different from the "membranous web," where the HCV replication complexes accumulate to show stronger expression of